

Understanding Evolution of NSW Coastal Dunefields Using LiDAR-Derived Dune Crest Mapping



Seal Rocks dunefield (October 2016)



Stockton Beach dunefield (May 2016)

William Farebrother, BSc (Hons)

Department of Environmental Sciences

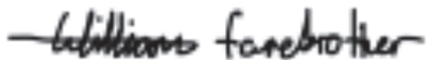
Faculty of Science and Engineering, Macquarie University

This thesis was submitted in accordance with the
requirements of the Masters of Research Degree

10 October 2016

Declaration

I hereby declare that this thesis has not been previously submitted to any other institution or university for a higher degree. Except where otherwise acknowledged, this thesis is comprised entirely of my own work.

A handwritten signature in black ink that reads "William Farebrother". The signature is written in a cursive style with a horizontal line extending from the start of the name.

William Farebrother 10/10/16

Acknowledgements

First and foremost, I would like to thank Paul Hesse for his constant and unwavering support and guidance throughout the year. Thanks to Ian Goodwin for his co-supervision and help acquiring the LiDAR datasets. Thanks to Kira Westaway for showing me the ropes on how to take pOSL samples and run them back in the lab. Thanks to Mark Lackie for generously lending me your dGPS for use in the field (I promise to get it working next time).

Thanks to Tim Ralph for navigating me through the Masters of Research process. A special thanks to the rangers from the Seal Rocks (Myall Lakes National Park) and Worimi Conservation lands for allowing me access to the National Parks and permission to dig.

I would like to thank my office mates (Sam, Liam, Daniel, Jack and Mac) for the support, camaraderie throughout the year and all the useful information and help acquired through the brains trust. I wish you all a bright future! Thanks again to Liam for coming out in the field with me to collect the endless samples and the digging of sample pits.

Finally, I would like to thank my family and friends, for the endless support and understanding throughout the year.

Abstract

Studies have highlighted the need to understand how coastal dunefields evolve over time, to inform their future management. This thesis explores how sand supply can influence the formation and evolution of coastal dunefields through the analysis of LiDAR-derived DEMs. This thesis presents two papers; (1) exploring long-term evolution of NSW coastal dunefields, and (2) exploring the short-term migration patterns within the southern Newcastle Bight. Through volumetric analyses, utilising a novel automated dune crest mapping approach, it was found that the Seal Rocks dunefield experienced a decrease in sediment supply during the late Holocene, while Booderee and the Newcastle Bight experienced an increase in supply. We suggest that over the late Holocene, small variations in wave climates supplying sediment to these dunefields may have resulted in this variability however any such fluctuation cannot be reliably detected from the orientation of the transgressive dunes. Short-term dune migration (2007-2013) within the southern Newcastle Bight was found to be dominated by the SW-NE oriented dunes moving towards the NW, and the NW-SE oriented dunes towards the NE.

Table of Contents

Declaration.....	ii
Acknowledgements.....	iii
Abstract.....	iv
List of Software Packages and Datasets.....	vii
List of Acronyms.....	vii
Chapter 1: Introduction	1
1.1. Factors affecting dunefield evolution	1
1.1.1 Coastal foredune and dunefield evolutionary pathways.....	2
1.2. Morphology.....	6
1.3. Aims and Hypotheses.....	8
1.4 Thesis structure.....	8
Chapter Two: LiDAR derived analysis of the evolution three key NSW coastal dunefields during the Holocene.	9
2.1 Abstract:.....	10
2.2 Introduction	10
2.3 Regional Setting	12
2.3.1 Regional sea level change	12
2.3.2 Regional sediment supply	13
2.3.3 Seal Rocks (SR) dunefield	14
2.3.4 Newcastle Bight (NCB) dunefield.....	14
2.3.5 Booderee dunefield	15
2.4 Method Background	17
2.4.1 The crest mapping approach.....	18
2.4.2 Relative chronology and depth of the inter-dune surface.....	20
2.4.3 Volumetric Analyses.....	22
2.4.4 Statistical Analysis of Dune Orientation	22
2.5 Results	23
2.5.1 Geomorphic Mapping	23
2.5.2 LiDAR Accuracy	25
2.5.3 Automated Crest mapping	25
2.5.4 Dune Orientation: azimuth of maximum slope (within 10 m of dune crest)	26
2.5.5 Dune Height	30
2.5.6 Portable OSL and degree of pedogenesis	31
2.5.7 Area-normalised volumes per dune group	33
2.5.8 Embayment slope	35

2.6 Discussion.....	35
2.7 Conclusions	38
2.8 Acknowledgements.....	39
2.9 References	39
Chapter 3: Short-term migration of southern Newcastle Bight dunefield detected by multi-temporal LiDAR.....	40
Abstract:.....	40
3.1 Introduction	41
3.2 Regional Setting	42
3.3 Methods	43
3.4 Results	44
3.4.1 LiDAR Accuracy	44
3.4.2 Crest mapping	45
3.4.3 Volumetric analysis of sand movement	46
3.4.4 Resultant Drift Direction (RDD).....	46
3.5 Discussion.....	48
3.6 Conclusions	49
3.7 Acknowledgements.....	50
Chapter 4: Thesis conclusions and recommendations for further study.....	50
Chapter 5: References.....	52
Chapter 6: Appendices.....	58

List of Software Packages and Datasets

Software Package	Revision
ArcGIS	10.3
ENVI	5.2.1
GRASSGIS	7.0.3
R and R Studio	3.3.1 (0.99.903)
movMF (Mixtures of von Mises-Fisher Distributions)	0.2-0

Dataset	Year
Bulahdelah 1x1 m DEM	2013
Port Stephens 1x1 m DEM	2012
Hunter 2x2 m DEM	2007
Raymond Terrace 1x1 m DEM	2013
Nowra 1x1 m DEM	2010
Smartline 100k	Australian Coastal Smartline Geomorphic and Stability Map, version 1 (2009)
Australian Bathymetry and Topography dataset	2009

List of Acronyms

Acronym	Meaning
LiDAR	Light Detection and Radar
DEM	Digital Elevation Model
SR	Seal Rocks
NCB	Newcastle Bight
RDD	Resultant Drift Direction
DP	Drift Potential
ENE	East North East
WNW	West North West
NW	North West

Chapter 1: Introduction

Coastal dunefields are invaluable sources of palaeoclimatic information (Bristow *et al.*, 2007; Gracia *et al.*, 2006; Otvos, 2000; Tamura, 2012), habitats for endangered flora and fauna, and regions of significant cultural importance (Gracia *et al.*, 2006). Many are now protected under State and Federal law through being designated as parts of National Parks. Several international studies have highlighted a need to understand how these systems evolve both spatially and temporally, to improve the long-term viability of rehabilitation processes undertaken to protect these systems into the future from the increasing threats of urbanisation and climate change (Carter, 1991; Hesp, 2013; Lithgow *et al.*, 2013; Luna *et al.*, 2011; Mitsova *et al.*, 2005; Rust and Illenberger, 1996; Yan and Baas, 2015). To this end, this thesis aims to explore the evolution of coastal dune systems by analysing the morphology of the dunes measured with unprecedented precision and detail by airborne Light Detection and Ranging (LiDAR) surveys.

This thesis is separated into two related but distinct papers. The first paper explores the evolution of three New South Wales (NSW) dunefields since their formation during the Holocene through the use of a novel automated crest mapping approach applied to LiDAR DEMs which provides the basis of subsequent morphometric and volumetric analyses. These dunefields include those found within the Bherwerre (Booderee), Newcastle Bight (NCB) and Seal Rocks (SR) embayments. The second paper explores the short-term evolution of the southern end of the NCB through the use of multi-temporal LiDAR. This second paper may offer important insights for the management of the currently active foredune, a system which is in close proximity to current urban expansion and mining activities. In both papers we analysed measures of morphology including orientation, height and their relationship with dune size and location within the embayment. This introductory chapter will briefly explore the various factors affecting dunefield evolution and dune morphology.

1.1. Factors affecting dunefield evolution

Three important factors influencing the formation and evolution of coastal dunefields have been identified: sand supply (driven by coastal orientation and wind and wave climates) (Aagaard *et al.*, 2004; Bauer *et al.*, 2009; Hesp, 2012; Short, 1988; Short, 2010b; Short and Hesp, 1982), vegetation (density, diversity and long-term stability) (Carter, 1991; Hesp, 2004; Keijsers *et al.*, 2015; Luna *et al.*, 2009; Nield and Baas, 2008; Yan and Baas, 2015) and sea level oscillation/change (Carter, 1991; Hesp, 2013; Lees, 2006; Luna *et al.*, 2011). The possible relationships between these factors are shown in Figure 1.

Sand supply has long been recognised as an important factor in determining the evolution of the morphology coastal dunes and over extended periods the evolution of coastal dunefields (Bauer and Davidson-Arnott, 2003; Bauer *et al.*, 2009; Goodwin *et al.*, 2006; Hesp, 2013; Short, 1988). Early works undertaken by Hack (1941) concluded that there are three main prerequisites for dune formation;

- (1) A sand supply or source,
- (2) A persistent wind strong enough to mobilise sand, and,
- (3) A place for the mobilised sand to be deposited.

The deposition of sand can be aided by the presence of vegetation that increases surface roughness resulting in the slowing down of the wind resulting in increased deposition of sand and restricting its re-entrainment (Baas, 2002; Luna *et al.*, 2009; Luna *et al.*, 2011; Nield and Baas, 2008; Yan and Baas, 2015).

Within a coastal environment the added factor of wave climates is introduced. Durán and Moore (2013) hypothesised that the beach type and size of waves has a significant effect on vegetation dynamics whereby the higher waves found on dissipative beaches increase the disturbance to foredune species causing foredune landward migration and larger dunes than those of reflective beaches where smaller waves dominate. Vegetation disturbance can also be caused by high sediment supply causing vegetation dieback, increased soil salinity and salt spray (Hesp, 1991; Kidd, 2001). A recent coastal dune genesis model by Luna *et al.* (2011) concluded that vegetation and sediment supply/influx greatly affect the formation and dynamics of dunefields within coastal environments. They found that when the maximum vegetation height (H_v) is small (~20 cm) only a small amount of sediment is trapped at the beach. This results in small (up to 2 m) crescentic dunes emerging from the sand sheet with increasing height and distance from the beach face. With higher H_v the efficiency of sand accumulation by the vegetation increases. At $H_v = 50$ cm dunes with a height of ~6 m and trailing ridges are formed; increasing to 7-10 m dunes when $H_v = 8$ m. They also concluded that with an increase in bare beach width (fetch) came an increase in sand accumulation and dune growth resulting in a smaller dune spacing, supporting findings of such studies as Bauer and Davidson-Arnott (2003) and Bauer *et al.* (2009). Durán and Moore (2013) found that vegetation zonation is the primary control on the maximum size of foredunes whilst sand supply to the dunes determines the formation timescale.

1.1.1 Coastal foredune and dunefield evolutionary pathways

Two seminal papers by Hesp (2013, 2002) highlight the various evolutionary pathways that coastal foredunes and dunefields are likely to take based upon sea level, sand supply and vegetation (Table 1 and 2). It is important to note that within each dunefield variability can exist and different parts of the dunefield and/or foredune complex can be following different pathways concurrently.

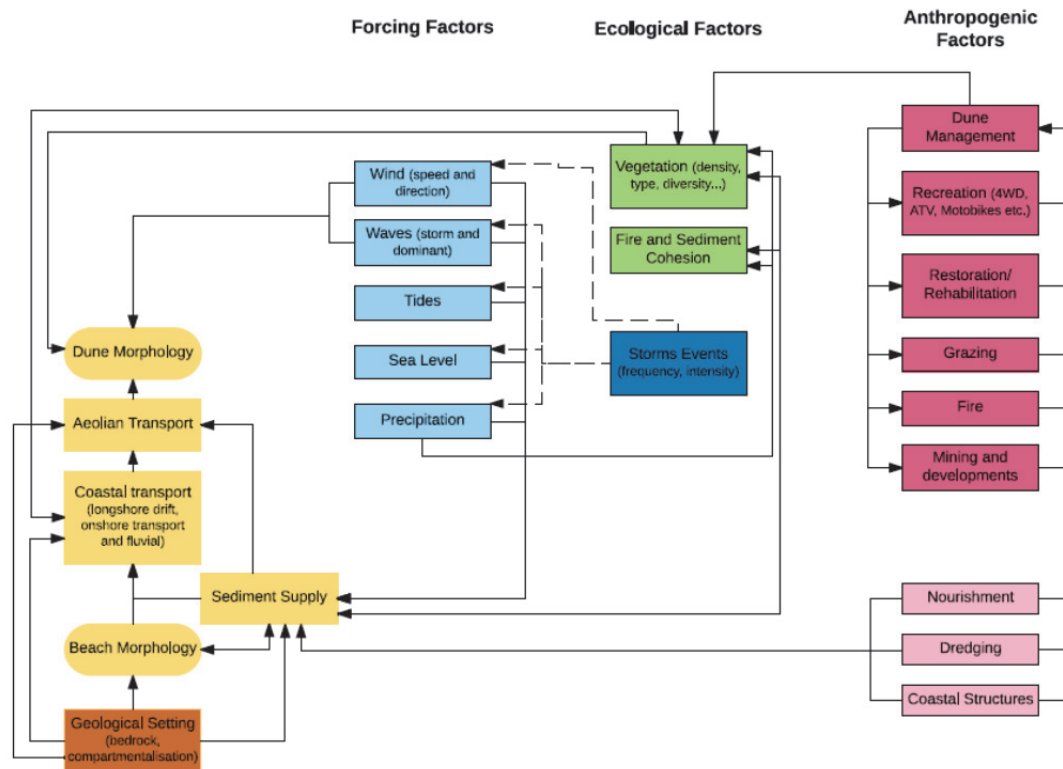


Figure 1: Factors affecting coastal dune morphology. Note: Solid lines represent continuous relationship whilst dashed lines represent episodic relationships. Adapted from Pye et al. (2007) and Del Angel (2012).

Table 1: Changes in foredune morphology with sea level change. Adapted from review undertaken by Hesp (2002).

Sea level	Beach width	Sediment supply	Vegetation	Dune Morphology	Effect of increase storminess
Fall	<i>Increases</i>	<i>Increases-dependent upon beach slope and size of sea level fall</i>	<i>If able to keep up with increased sediment supply</i>	<i>Dune grows vertically and laterally</i>	<i>Minimal: vegetation readily able to recover and stabilise</i>
			<i>Dune vegetation swamped by increased supply</i>	<i>Sediment bypasses foredune resulting in blowouts, foredune may breakdown</i>	<i>Variable: where vegetation is still present potential recovery; otherwise foredune breakdown may occur</i>
			<i>Pioneer vegetation absent</i>	<i>Dune instability occurs forming blowouts, parabolic and transverse dunes</i>	<i>High: no vegetation to stabilise sediment</i>
Rise	<i>Decreases</i>	<i>Decreases-dependent upon beach slope and size of sea level rise</i>	<i>Vegetation unable to stabilise due to erosion of stoss slope. But colonises upper slope of dune</i>	<i>Blowouts occurs, Dune retreats landward and grows taller</i>	<i>High: Increased landward retreat.</i>
			<i>Vegetation unable to stabilise eroding dune</i>	<i>Foredune is scarped by rising sea level and storms. Foredune destabilises and forms blowouts, parabolic, sand sheets and/or transgressive dunefields.</i>	<i>High: due to lack of stabilisation by plants increased storminess speeds up destabilisation.</i>
		<i>Despite sea level rise sediment supply remains high</i>	<i>Vegetation able to stabilise foredune</i>	<i>Progradation through formation of repeated foredunes results in beach ridge sequence being formed</i>	<i>Low-moderate: scarping of most seaward foredune may occur but should stabilise quickly</i>

Table 2: Transgressive dune/field evolution under three key scenarios and their associated characteristics. Adapted from Hesp (2013).

Scenario	Stages	Sand supply	Key evolution sequence (temperate to tropical)
1. Development from the backshore	I – Mobile and active, transverse and barchanoid precipitation ridge forming as dune moves downwind	High	Barchanoids and transverse dominate, but are typically complex. Large range of bed forms, swales and flats present, poorly developed deflation plains. Vegetation may be present in interdunes.
	II – Continual migration, interdunes may be at water table or bedrock/calcrete and/or colonised by vegetation, deflation plain may form		Precipitation ridge surrounds most upwind region of dune/field, stabilised form depends on rate of stabilisation. Multiple phases might form multiple crenate ridges , or a new phase might cannibalise the older.
	III – Larger deflation plains, trailing ridges, slacks and wetlands, parabolic dune formation		Sediment supply variability may create multiple phases, or, a foredune might form and then break down during period of lower supply.
	IV – Largely or fully vegetated, unorganised network of dunes		Dune/field migrates, foredune develops (either completely and cuts of sediment supply, or spatially variable and blowouts continue to form) Deflation plain is developed. Migrating dune leaves behind a complex topography of trailing ridges, parabolics and remnant dunes.
	V – Blowout formation and reworking		Parabolic dunes form where migration is partially stabilised by vegetation. Can remain active for an extended period. Usually single phase. May then stabilise (sometimes only forming a single precipitation ridge)
2. Development from foredune or dune erosion	I – Foredune breakdown, scarping, overwash fans and sheets, blowouts, sandsheets and ramps	Moderate to high	Scenario described involves a retrograding coastline. Supply (high or low) is determined by the volume of sediment previously in the foredune or dune/field.
	II – If sheets are formed with foredune breakdown, sheets merge into transgressive dune, remnant knobs left at stabilised foredune location/s. If blowouts formed with foredune breakdown, they may evolve into a parabolic morphology then merge into a transgressive sheet (or not become transgressive at all)		Continuing retrogradation can cause multiple phases of dunes to migrate over pre-existing forms. Forms include parabolic and other transgressive dune forms.
	III – Continual migration then eventual stabilisation. Following similar pattern to stage III scenario 1 . Foredune may form and cut off sediment supply to inland.		Migration resulting from cannibalising of smaller inland features (with limited supply from beach) will be less pronounced – thinner sand sheet and shallow saucer blowouts. Nekha can develop on the surface of the sheet. If vegetation growth is allowed to persist, the dune/field may stabilise into a hummocky terrain. Note that dunes forming in this way may be further altered/cannibalised by episodes of the same destructive processes which first initiated the transgression.
3. Development from parabolic dunes	I – Parabolic dunes expand laterally and merge, trailing ridges break up, expanding depositional lobes and discontinuous precipitation ridges II – Parabolics merge and evolution then follows similar pattern to scenario 1.	-	

The evolution of the field is dependent upon sediment supply and climate (Hesp, 2013). High sediment supply often leads to a complex system with multiple episodes of dune formation; however if the sediment supply slows or stops a deflation plain or basin can form upwind/seaward of the dunefield (Hesp, 2013). Under a low sediment regime the dunefield may remain active for some time and then be stabilised by vegetation, often resulting in a simpler dune field. Hesp (2013) also noted that blowouts, parabolic dunes and transgressive dunefields all cannibalise pre-existing dunes and the current dune/dunefield morphology is often an incomplete or partial copy of the original. This can be seen in such systems as the NCB where the current (3rd generation) dunes are cannibalising the older beach ridges in the north and 2nd generation dunes in the south.

Variations of the factors explored above may help explain the significant morphological variability seen between and within dunefields along the NSW coast. Although this study explores the effects of sand supply on the evolution of these systems, it is important to note that the influences of vegetation and sea level change are intrinsic to these systems and as such they cannot be removed from any analysis undertaken. However, as sea level change is a regional process, the variability of its effects are considered to be minimal between the study sites (Lewis *et al.*, 2013). In contrast, vegetation variability operates across a wide range of scales (both spatially and temporally) so its effects can vary significantly within and between dunefields (Hesp, 2004; Hesp, 2013; Luna *et al.*, 2009). Assessments of possible vegetation dynamics within this study will be limited to the possible effect of vegetation upon the dune morphology seen within each dunefield.

To date, research into dunefield evolution around the world has been dominated by the study of the morphology of arid dunefields through aerial and remotely-sensed data (Al-Masrahy and Mountney, 2013; Bishop, 2010; Blumberg, 2006; Bullard *et al.*, 1995; Derickson *et al.*, 2008; Ewing and Kocurek, 2010; Ewing *et al.*, 2006; Telfer *et al.*, 2015). Many coastal dunefields experience high precipitation rates, particularly in temperate east coast settings. Consequently, dense vegetation often obscures the surface topography making remotely sensed imagery less effective for exploring dunefield morphology. Studies such as Bailey and Bristow (2004) used aerial photographs to map largely unvegetated parabolic dunes using digitisation within GIS software. Similarly, Thom *et al.* (1992) had to rely upon the analysis of the larger features that were visible in aerial photographs and costly site visits to explore these systems. Similarly expensive and time consuming, Andrews *et al.* (2002) utilised repeated total station surveys to manually construct high resolution DEMs from point clouds to study short-term evolution of a foredune. More recently, studies such as Mitsova *et al.* (2004) integrated multi-temporal topographic mapping (ranging from topographic maps, LiDAR and Differential GPS surveys) to explore dune evolution thereby illustrating the importance of repeated surveys of these types of systems.

Hugenholtz *et al.* (2012) review of remote sensing and spatial analysis of dunes concluded that DEM data offers one of the most important media for future research into the analyses of dune topography and dunefield patterns.

Recently the NSW Department of Land and Property Information (LPI) released DEMs from high resolution LiDAR surveys along the NSW coast to explore the potential effects of sea level change (NSW Department of Planning, 2008). These surveys provided high resolution and high accuracy Digital Elevation Models (DEMs) which depict the bare earth surface, digitally 'stripped' of its vegetation covering. These datasets offer a unique and previously unseen look into the morphologies of several key coastal dunefields and form the foundation of the analyses included within this study.

1.2. Morphology

Morphological assessments offer important insights into the evolution of dunefields; especially when supplemented by dating methods (Bristow *et al.*, 2007; Varma *et al.*, 2014). The morphology of an individual dune is intrinsically linked to the dynamics of sand supply used to form it (Hack, 1941; Luna *et al.*, 2011). Variable sand supply and vegetation allow dunes to grow and occasionally change type (Hesp, 2002; Hesp, 2013; Keijsers *et al.*, 2015; Luna *et al.*, 2011; McKee, 1979; Yan and Baas, 2015).

Modelling studies undertaken over the past decade have illustrated that dunes and dunefields form and evolve due to variations in the sediment supplied to them and variability in the vegetation cover that helps to stabilise them (Aagaard *et al.*, 2004; Baas, 2002; Baas and Nield, 2007; Baas and Nield, 2010; Barchyn and Hugenholtz, 2012a; Durán and Moore, 2013; Luna *et al.*, 2011; Nishimori and Tanaka, 2001). Sediment supply has also been intrinsically linked to dune height and volume (Bauer and Davidson-Arnott, 2003; Houser and Mathew, 2011), whereby an increase in sediment supply leads to the formation of higher and more voluminous dunes and/or a greater number of dunes. Parabolic dune formation has been linked to instability caused by either a partial stabilisation by vegetation coverage and/or a high sediment supply; whereby increased sediment supply restricts vegetation establishment resulting in a partial stabilisation of the dune downwind (Hesp, 2002; Hesp, 2013).

Hack (1941) concluded that dunes can be ordered by sand supply: transverse dunes have the largest sand supply which results in little to no vegetation being able to survive, parabolic dunes have a moderate supply of sand and longitudinal dunes have the lowest sand supply. Subsequently, Wasson and Hyde (1983) revisited this relationship for desert dunes finding that sand thickness and directional variability of sand-moving winds as being most important to dune type, whilst wind strength and sediment particle size are less important. They also noted that vegetation has an ambiguous role, concluding that "vegetation is obviously significant in the parabolic dune form but it is not clear whether, apart from that, it significantly affects the development of one dune type in preference to another..."

(Wasson and Hyde (1983), page 339). Within a coastal environment it is important to note that sand supply is potentially more complex than in an arid environment as the effects of wave climates become integrated. Yan and Baas (2015) highlighted that the formation and evolution of parabolic dunes is dependent upon vegetation supporting the findings of earlier works by (Hack, 1941; Hesp, 2002; McKee, 1979). They noted that parabolic dunes can develop from the partial stabilisation by vegetation of mobile barchan and transverse dunes (supporting the findings of Barchyn and Hugenholtz (2012b)). It is important to note that if dunes are not stabilised (by vegetation or other forms of armouring, such as surface crusts) the dune may be reworked and therefore represent an integration of the original formation conditions and any post-genesis reworking (usually in the form of 'defects') (Kocurek and Ewing, 2005). Dune type is intrinsically linked to the integration of sand supply, vegetation colonisation and climatic factors including dominant wind direction and precipitation. Consequently dune morphology and its relationship with vegetation and sand supply can offer important insights into the factors that governed the dunefield in its formation and subsequent reworking, and can help to tell the story of what may have caused the dunefield structure we see in the system today.

Table 3: Measures of dune morphology and their potential to offer insights into dunefield evolution. Those bolded include measures explored within this study.

Measure	Attribute (unit)	Method of extraction	Potential insight
Dune form	Parabolic Transverse Annular Foredune/Beach ridge	Crest orientation, Slip face orientation	Dune stability, forming wind direction/s and signs of reworking Relative sand supply
Size	Volume (km ³)	ArcMap raster analysis (Map Algebra) informed by inter-dune depths and vertical LiDAR accuracy.	Sand supply
	Height (m)	Average height above nearest interdune	Sand supply
Density	Number of dunes or crest length per km ²	Number of discrete dune polylines within a km ² as determined by a fishnet	Sand supply
Slope	Degree (°)	Lee and stoss slopes- averaged slope taken from perpendicular transects at set interval using transect tool developed by Ferreira (2014).	Degree of dune stability
Dune/coastal orientation	Degree (°)	Measured from upwind coastline as determined from dune orientation.	Formation/reworking dominant wind direction/s
Compartment size	km ²	Measured from upwind compartment boundary and closest point of -50 b.s.l. barometric line.	Sand supply
Cross-cutting relationships		Analysis of crest junctions	Relative age/variation in wind/sand supply
Superposition		Vertical relationships/compound dune features	Relative age/degree of reworking
Defects	Density (#/km)	Statistical analysis of number of crestlines that are less than a set cut off value	'Maturity', age

There is a general belief that sediment supply to the NSW coastline has significantly decreased since the Holocene marine transgression, when a large amount of sediment was supplied to the coast, forming the coastal barriers seen today (Davies, 1986, Short, 1988, Short and Hesp, 1982). This decrease was likely due to the exhaustion of sand stored on the inner continental shelf and a significant

decrease in terrigenous fluvial input (Davies, 1986, Short, 1988, Short and Hesp, 1982). This is thought to be a significant contributing factor to the stabilisation of many dunefields along the NSW coast during the late Holocene. Studies have also shown that during the late Holocene, winds derived from the south and southeast were responsible for the formation and reworking of the NSW coastal dunefields (Goodwin *et al.*, 2006; Hesp and Thom, 1990; Thom *et al.*, 1992). In contrast some recent studies undertaken on regressive coastal strandplains have suggested that sediment supply has increased in the north coast of NSW (Goodwin *et al.*, 2006) or stayed relatively constant (in the south coast of NSW) during the late Holocene (Oliver *et al.*, 2015). The possible measures of dune morphology and those utilised in this study are shown in Table 3.

1.3. Aims and Hypotheses

This thesis will use recent advances in remote sensing technology to explore the variability in transgressive dunefield morphology and volume along the NSW coast. We will explore dune morphology at these study sites and (i) identify possible patterns in the rate of late Holocene sediment supply (Davies, 1986; Goodwin *et al.*, 2006; Oliver *et al.*, 2015; Short, 1988; Short and Hesp, 1982), and (ii) whether localised areas of enhanced sediment supply are characterised by blowout and parabolic dune features indicative of greater instability (Hack, 1941; Hesp, 2002; Hesp, 2013; McKee, 1979). (iii) Additionally, this thesis will use LiDAR derived DEMs to quantify the rates and major migration directions of the modern dunes in the southern NCB and the relationship with winds above-threshold values. This will offer crucial insights into how the dunefield developed and help to inform management strategies to protect cultural heritage values and urban infrastructure in the path of the currently migrating dunes which have been identified as having great importance to the park (Worimi Conservation Lands, 2015). (iv) A supplementary aim of this thesis is to develop a new automated crest mapping approach to allow morphometric analysis to support these investigations. Paper one (Chapter 2) will explore aims (i), (ii) and (iv) whilst paper two (Chapter 3) will cover aim (iii).

1.4 Thesis structure

This chapter has introduced the background and key aims of this study. The subsequent chapters of this thesis consist of two separate but related draft papers to be submitted for publication. The first paper explores the evolution of three key coastal NSW dunefields since their formation during the Holocene. The second paper focusses on the short-term evolution of the southern NCB embayment through the use of repeated overlapping LiDAR surveys. Both papers are structured as stand-alone journal articles and as such some unavoidable overlap in content may occur, but this overlap will be kept to a minimum. The final chapter will integrate the findings of both papers and offer recommendations for future study.

Chapter Two: LiDAR derived analysis of the evolution three key NSW coastal dunefields during the Holocene.

Purpose: This chapter presents original research that has been entirely undertaken within this Masters by Research year (January 2016-October 2016). The chapter provides a journal paper draft including an Abstract, Introduction, Methods, Results and Discussion related to the long-term evolution of three coastal dunefields within NSW and the creation of a novel automated crest mapping approach. This paper has the objective of exploring aims (i), (ii) and (iv). There has been no high-resolution analysis of dunefield morphology of these key NSW dunefields and this research will underpin future research and management of these systems. The automated crest-mapping approach outlined in this paper offers a largely objective and replicable method of deriving crestlines from DEMs and may contribute to dunefield morphological and evolution research.

Format: In accordance with the Macquarie University policy for higher degree research thesis by publication¹ this chapter has been written for submission to a peer-reviewed journal. Repetition and any referencing and stylistic inconsistencies have been minimised to facilitate the thesis examination process. Supplementary material and references referred to in the paper are provided in the reference list and appendices at the end of the thesis, and are intended to become the references and supplementary material provided in the published version of this paper.

Author contributions:

William Farebrother (W.F.): carried out fieldwork and pOSL sampling with P.H. and L.T., conducted laboratory and mapping works, analysed all the data, designed all figures and tables, wrote and edited the paper.

Paul Hesse (P.H.): helped develop the study and conduct fieldwork and sampling with W.F., provided advice and helped to edit the paper and supervised W.F. in the research.

Liam Turner (L.T.): helped to carry out fieldwork and sampling with W.F. and created and helped adapt R code for the statistical analyses of orientation undertaken within this research.

Kira Westaway (K.W.): Helped instruct W.F. on the laboratory methods involved in undertaking pOSL analysis.

¹ The Macquarie University policy for thesis by publication states that a thesis may include a relevant paper or papers that have been published, accepted, submitted or prepared for publication for which at least half of the research has been undertaken during enrolment. The papers should form a coherent and integrated body of work. The papers are one part of the thesis, rather than a separate component (or appendix) and may be single author or co-authored. The candidate must specify their contribution and the contribution of others to the preparation of the thesis or to individual parts of the thesis in relevant footnotes/endnotes. Where a paper has multiple authors, the candidate would usually be the principal author and evidence of this should appear in the appropriate manner for the discipline. MQ Policy: http://www.mq.edu.au/policy/docs/hdr_thesis/policy.html

2.1 Abstract:

Studies have highlighted the need to understand how coastal dunefields evolve over time, to inform their future management. This study explores how sand supply can influence the formation and evolution of coastal dunefields through the analysis of LiDAR-derived DEMs. Through volumetric analyses of three NSW coastal dunefields, utilising a novel automated dune crest mapping approach, it was found that the Seal Rocks dunefield experienced a decrease in sediment supply during the late Holocene, while Booderee and the Newcastle Bight experienced an increase in supply. We suggest that over the late Holocene, small variations in wave climates supplying sediment to these dunefields may have resulted in this variability however any such fluctuation cannot be reliably detected from the orientation of the transgressive dunes.

2.2 Introduction

Coastal dunefields are invaluable sources of palaeoclimatic information (Bristow *et al.*, 2007; Gracia *et al.*, 2006; Otvos, 2000; Tamura, 2012), habitats for endangered flora and fauna, and regions of significant cultural importance (Gracia *et al.*, 2006). They are often protected under State and Federal law as parts of National Park systems. Several international studies have highlighted a need to understand how these systems evolve both spatially and temporally, to help improve the long-term viability of rehabilitation processes undertaken to protect these systems from the increasing threats of urbanisation and climate change (Carter, 1991; Hesp, 2013; Lithgow *et al.*, 2013; Luna *et al.*, 2011; Mitasova *et al.*, 2005; Rust and Illenberger, 1996; Yan and Baas, 2015). Coastal dunefield systems/barriers have also been identified as buffers to storm surges (Kidd, 2001; Montague, 2008). This paper aims to: (i) identify possible patterns in the rate of late Holocene sediment supply which has been shown to vary along the NSW coastline during this period (Davies, 1986; Goodwin *et al.*, 2006; Oliver *et al.*, 2015; Short, 1988; Short and Hesp, 1982). (ii) Investigate whether dune morphology can reveal spatial and temporal variation in sand supply (Hack, 1941; Hesp, 2002; Hesp, 2013; McKee, 1979). (iii) Introduce a novel automated crest mapping approach to allow morphometric analysis to support these investigations (i), (ii).

Three important factors influencing the formation and evolution of coastal dunefields have been identified: sand supply (driven by coastal orientation and wind and wave climates) (Bauer *et al.*, 2009; Hesp, 2012; Short, 1988; Short, 2010b; Short and Hesp, 1982), vegetation (density, diversity and long-term stability) (Carter, 1991; Hesp, 2004; Keijsers *et al.*, 2015; Luna *et al.*, 2009; Nield and Baas, 2008; Yan and Baas, 2015) and sea level oscillation/change (Carter, 1991; Hesp, 2013; Lees, 2006; Luna *et al.*, 2011). Hesp (2013) has summarised the main evolutionary pathways that coastal transgressive dunefields are known to exhibit including (1) development from the backshore, (2) development from

foredune or dune erosion and (3) development from parabolic dunes. Hack (1941) concluded that desert dunes can be ordered by sand supply: transverse dunes have the largest sand supply which results in little to no vegetation being able to survive, parabolic dunes have a moderate supply of sand and longitudinal dunes have the lowest sand supply. More recently, Wasson and Hyde (1983) revisited this relationship for desert dunes finding that sand thickness and directional variability of sand-moving winds as being most important to dune type, whilst wind strength and sediment particle size are less important. They also noted that vegetation has an ambiguous role, concluding that “vegetation is obviously significant in the parabolic dune form but it is not clear whether, apart from that, it significantly affects the development of one dune type in preference to another...” (Wasson and Hyde (1983), page 339).. In coastal environments, Aagaard *et al.* (2004) found that the ‘welding’ of bars onto the beach has a significant role on sand supply during low tide to the landward dunes and subsequent morphological evolution.

To date our understanding of these systems has been restricted by the fact that they are often areas of dense vegetation cover which has significantly inhibited the ability of remotely sensed imagery to reveal details of dune morphology. This has resulted in the reliance upon costly site visits and/or creation of conceptual models to explain dunefield formation and evolution. Additionally, most available Digital Elevation Models (DEMs) have coarse resolution which may not fully resolve small dunes, even if bare of vegetation (Blumberg, 2006). Internationally, the use of airborne Light Detection and Ranging (LiDAR) surveys has been shown to offer unparalleled glimpses into how these systems evolve and their morphology at a given time (Houser and Mathew, 2011; Levin *et al.*, 2014; Mitasova *et al.*, 2005; Woolard and Colby, 2002). DEM data remains one of the most important avenues for future research into the spatial analysis of dunes (Hugenholtz *et al.*, 2012). The analysis of point cloud used to construct the LiDAR-derived DEM can be used to adaptively remove returns (points) that coincide with vegetation and can be used to explore both the morphology of dune features and the vegetation which helps to stabilise them (Doyle and Woodroffe, 2015).

This paper will explore the evolution of three transgressive dunefields along the NSW coast using LiDAR derived DEMs. These dunefields were selected for this study because they all reside on high energy dissipative coastlines, have similar coastal orientations and yet have vastly different morphologies. Along the NSW coastline, dunefields have formed in locations where shoreline orientation and, wind and wave climates have combined to allow significant quantities of onshore sediment transfer from the continental shelf during the Holocene marine transgression (HMT). This has resulted in the formation of extensive coastal dunefields where accommodation space allowed deposition (Short, 2010b). The Seal Rocks (SR) and Newcastle Bight (NCB) dunefields are two of only

a handful of coastal dunefields along the NSW coastline which have been extensively studied and have underpinned seminal works into the evolution of coastal dunefields (Thom *et al.*, 1994; Thom, 1983; Thom *et al.*, 1981; Thom *et al.*, 1992; Thompson, 1981). All three field sites have also been singled out as regions of significant cultural and natural importance becoming part of the national parks system. Recently the NSW Department of Land and Property Information (LPI) released DEM products from high resolution LiDAR surveys along the NSW coast to explore the future effects of climate change related sea level change (NSW Department of Planning, 2008). These surveys provided high resolution (1-2 m cell size) and high accuracy (0.15 m vertical RMSE and 0.6 m horizontal RMSE) DEMs which depict the bare-earth surface and consequently these datasets offer a unique and previously unseen look into the morphologies of several key coastal dunefields and form the foundation of the analyses included within this study. Table 1 highlights the acquisition dates and cell size of the DEMs utilised within this study. It is important to note that the RMSE values stated above were provided by (NSW Department of Planning, 2008) and consequently independent estimates of accuracy were made in the course of this study.

Table 1: LiDAR derived DEM datasets utilised in this study. Note: the Port Stephens DEM was resampled using Bilinear resample. See Appendix 1 for comparison between the different resample method outputs was used as it best represented the original data and is supported by the findings of (Tao *et al.*, 2008).

LiDAR DEM dataset	Year of Acquisition	Cell size (m x m)
Bulahdelah (SR)	2013	1 x 1
Port Stephens (Northern NCB)	2012	1 x 1
Hunter (Southern NCB)	2007	2 x 2
Nowra (Booderee)	2010	1 x 1

2.3 Regional Setting

The three dunefields chosen for this study include those found within Holocene coastal barriers of Seal Rocks (SR), Newcastle Bight (NCB) and Bherwerre Beach embayments (Booderee). Other than their similar orientation and contrasting morphologies these dunefields were also chosen as they have LiDAR DEM coverage and have been the focus of previous studies which have credited their formation to the Holocene marine transgression (HMT) (Thom *et al.*, 1994; Thom, 1987; Thom *et al.*, 1981; Thom *et al.*, 1992). This section will first explore features consistent between all field sites before exploring individual site-based regional settings.

2.3.1 Regional sea level change

A review of Holocene sea-level change in southeast Australia (Sloss *et al.*, 2007) concluded that post LGM sea levels were between -15 to -11 m below present mean sea level (p.m.s.l) between 9400-9000 cal. yr BP and then rose to -3.5 m by 8500. Present sea level was attained between 7900-7700 cal. yr BP and rose to +1.5 m by 7400 cal. yr BP. This sea level highstand lasted until ~2000 cal. yr BP and

was then followed by a slow regression to p.m.s.l (Sloss *et al.*, 2007). These dune systems were likely formed during the sea level highstand from sediments reworked from the flooded continental shelf (Davies, 1986, Short, 1988, Short and Hesp, 1982) and deposited over or against older Pleistocene barrier sands. Lees (2006) concluded that sea level change was the dominant trigger for broad scale dune development during the late Holocene within Australia. Due to their formation under higher sea levels than present it is improbable that the interface of the reworked Holocene sediments with the underlying Pleistocene sediment is significantly below p.m.s.l.

2.3.2 Regional sediment supply

Along the NSW coastline dunefield formation is found where drift aligned coastlines result in longshore transport and storage of sediment at the northern end of compartments (Short, 2010a). The degree of the embaymentisation in beaches along the NSW coastline generally decreases in a northward direction (Short, 2010a). Table 5 highlights the beach type, coastal orientation and inferred sediment supply of each of the study beaches.

There is a general belief that sediment supply to the NSW coastline has significantly decreased since the HMT, when a large amount of sediment was supplied to the coast, forming the coastal barriers seen today (Davies, 1986, Short, 1988, Short and Hesp, 1982). This decrease was likely due to the exhaustion of sand stored on the inner continental shelf and a significant decrease in terrigenous fluvial input (Davies, 1986, Short, 1988, Short and Hesp, 1982). This is thought to be a significant contributing factor to the stabilisation of many dunefields along the NSW coast during the late Holocene. In contrast, some recent studies undertaken on regressive coastal strandplains have suggested that sediment supply has increased in the north coast of NSW (Goodwin *et al.*, 2006) or stayed relatively constant (in the south coast of NSW) during the late Holocene (Oliver *et al.*, 2015).

Studies have also shown that during the late Holocene, winds derived from the south and southeast were responsible for the formation and reworking of the NSW coastal dunefields (Goodwin *et al.*, 2006; Hesp and Thom, 1990; Thom *et al.*, 1992).

Table 1: Study beach type, coastal orientation and inferred sediment supply. Adapted from (OzCoasts, 2015)

Beach Name	Study Site	Beach Length (km)	Beach Type	Embaymentisation	Coastal Orientation	Energy	Sediment Supply (dune volume)
Lighthouse	SR	1.95	TBR-RBB	0.71	159	High	Moderate
Treachery/Yagon	SR	1.85	RBB	0.77	163	High	High
Submarine/Fiona	SR	8.8	RBB	1.0	160	High	High
Stockton	NCB	32.7	RBB	N.D.- longshore drift est. 5000-23000 m ³ /year at southern end (Boleyn and Campbell, 1966)	151*	High	Very High
Bherwerre	Booderee	7.0	TBR-RBB	0.96	162	High	High

TBR= Transverse Bar and Rip RBB= Rhythmic Bar and Beach LTT= Low Tide Terrace

2.3.3 Seal Rocks (SR) dunefield

The SR dunefield is located c.190 km north of Sydney and is located within Myall Lakes National Park. The SR area receives a mean annual rainfall of 1226.3 mm/yr and average temperatures range from 14-23 °C (Bureau of Meteorology, 2016). The dunefield is almost entirely forested, except for some blowouts and parabolic dunes in the foredune complex. A series of geomorphological studies have been undertaken within the SR dunefield during the 1970s and 1980s (Thom *et al.*, 1994; Thom, 1983; 1981; 1992) whose findings all point to SR being formed during the Holocene as an extended activation event before being rapidly stabilised by vegetation. The recent stabilisation is inferred from the broad scale preservation of steepened slip faces within the dunefield. Radiocarbon dates have suggested that the precipitative ridge surrounding the upwind margin of the SR dunefield, Bridge Hill, was constructed during the late Holocene (between 3025 ± 135 yr B.P through to 1265 ± 135 yr B.P (Thom *et al.*, 1992).

Anthropogenic alteration of the dunefield includes sand mining operations within the northern part of Bridge Hill (Figure 1, a) in the northwest margin of the dunefield. Another smaller mining operation was undertaken in the sandsheet immediately behind the foredune complex behind Fiona Beach (Roy, 1999).

2.3.4 Newcastle Bight (NCB) dunefield

The NCB is c.130 km north of Sydney and is a 32 km dunefield located within the co-managed Worimi National Park and Worimi Conservation Lands. The NCB area receives a mean annual rainfall of 1126.7 mm/yr and average temperatures range from 12-23 °C (Bureau of Meteorology, 2016). A large part of the dunefield, the 'current generation', is bare and mobile and is currently the largest active coastal dunefield in NSW (Robson *et al.*, 1993). The older generations of dunes are currently well

vegetated. The dunefield has been highlighted as significant to Aboriginal cultural heritage with numerous artefacts and middens being found within the dunefield (Worimi Conservation Lands, 2015). Thom *et al.* (1992) undertook an in-depth study of the geomorphology of the NCB concluding that the dunefield was formed in three stages in the Holocene resulting in the formation of three generations of dunes on the Holocene barrier seen today (Figure 1, b). These generations are also the longest continuous Holocene (outer) barriers within NSW (Thom *et al.*, 1992).

The NCB has undergone the most anthropogenic alteration of the study sites. Alterations include a number of sand mines, increasing urban developments on the first and second dune generations and use of the southern end of the foredune as a military proving ground (Worimi Conservation Lands, 2015). All areas of visible anthropogenic alteration have been removed from the analyses undertaken within this study (with the exception of the volumetric analyses). These alterations are most prominent in the southern and inland areas in particular (Figure 1, b). Due to delays with permit processing and access limitations, only four soil sample pits were dug within the NCB. These pits cover the interface between the second and current generations; no pits were dug within the first generation of dunes.

2.3.5 Booderee dunefield

The Booderee dunefield is located 200 km south of Sydney and is located within the co-managed Booderee National Park, Jervis Bay Territory ACT. The Booderee area receives a mean annual rainfall of 1110.7 mm/yr and average temperatures range from 13-21 °C (Bureau of Meteorology, 2016). Thom (1987) suggested that the dunefield formed during the mid to late Holocene, inferred from shallow podzol soil development throughout the dunefield and two radiocarbon ages. It has been noted that the dunefield may have been mobilised as a result of grazing, fires and logging pressures, for an extended period following European settlement in the 1880s before being stabilised (Lindenmayer *et al.*, 2014). Consequently, during the 1960s-1970s a rehabilitation project was undertaken which included bulldozing the foredune and planting marrum grass, coastal wattle and Bitou Bush (Lindenmayer *et al.*, 2014). The levelling and colonisation largely stabilised the foredune and cut off sediment transport resulting in rapid stabilisation (evident in Figure 1, c). Only localised blowouts are currently evident in the south western end of Bherewerre Beach near the entrance of St Georges Basin (see Figure 1, c). The rehabilitated foredune has been removed from morphometric analyses undertaken within this project due to its significant anthropogenic alteration; however the blowouts and the remnant beach ridge sequence in the northeast have been included. Due to protracted permit issues no fieldwork was undertaken within the park and therefore the following analyses are purely desktop-based.

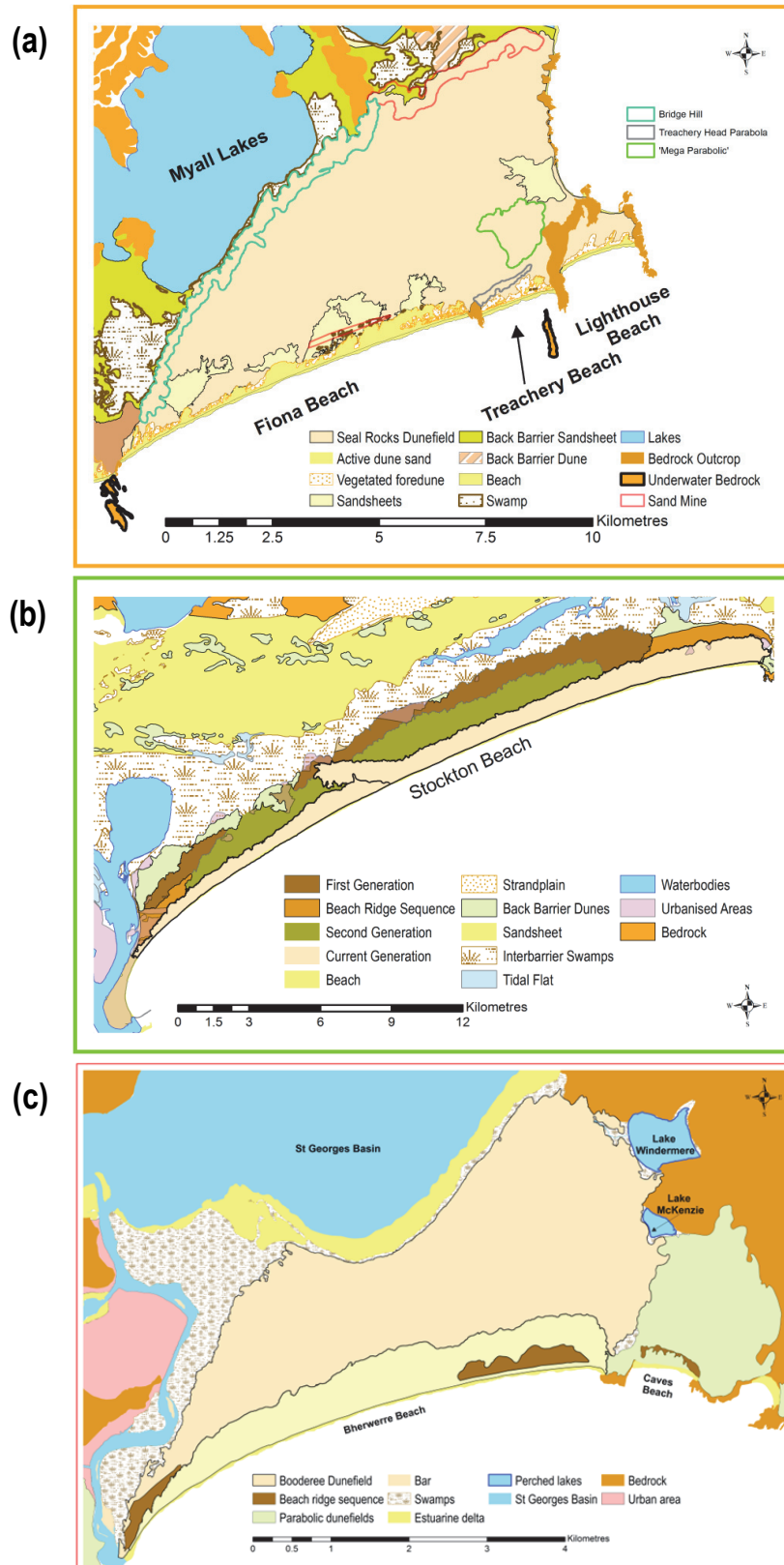


Figure 1: Geomorphic map of (a) Seal Rocks, (b) Newcastle Bight and (c) Booderee. Seal Rocks and Newcastle Bight geomorphic units/dune generations were modified from Thom *et al.* (1992). Booderee units/generations were informed by Thom (1987). The maps were modified by incorporating the analysis of aerial imagery and LiDAR derived DEMs.

2.4 Method Background

To date, morphological assessments of dunefields have largely focused upon inland arid dunefields as they have the advantage of regularly spaced dunes throughout broad-scale regions. This phenomenon is often referred to as self-organisation (Kocurek and Ewing, 2005) whereby a given wind regime will often produce a relatively simple dune-field pattern over extended periods of time. In this type of system, the dune morphology is determined by the interaction of dunes with the wind regime and dune-dune interactions (through collisions and wind deflection). The presence of small perturbations within the wind regime or wholesale change can cause 'defects' to form leading to a more complex pattern; however these defects have been found to move faster than the larger-scale morphology and become superimposed onto the larger system (Kocurek and Ewing, 2005).

Historically, the study of dunefield morphology has been undertaken through manually digitising or measuring dune crests from topographic maps and aerial photography (Bailey and Bristow, 2004; Bullard *et al.*, 1995; Derickson *et al.*, 2008; Wasson *et al.*, 1988). More recently, satellite imagery and DEMs have enabled dune crests to be digitised through tracing visible features using a georeferenced image/raster (Baitis *et al.*, 2014; Ewing *et al.*, 2006), edge detection algorithms undertaken on Landsat TM imagery (Telfer *et al.*, 2015) or DEMs (Swanson *et al.*, 2016), Fourier transform filters used on DEMs (Cazenave *et al.*, 2013) and Object Based Image Analysis (OBIA) using remotely sensed imagery (Vaz *et al.*, 2015). In arid environments, the regular spacing of dunes lends itself to methods which utilise crest wavelength such as Fourier analysis. In contrast, the wavelength between coastal dunes is highly variable (evident in the visual analysis of LiDAR imagery) and methods that utilise wavelength or a fixed window size are likely to ignore features which do not fit the 'representative wavelength' integrated into the model. Similarly, edge detection methods undertaken using aerial photographs and/or satellite imagery are significantly hampered by the obscuring effects of vegetation and are consequently often unsuitable for the study of many coastal dunefields. Likewise, edge detection methods undertaken on DEMs that rely on fixed window size filtering may ignore features filtered out during pre-processing. Manually derived dune crest mapping is plagued by the complexity of these systems but also adds user-based subjectivity and subsequently the results may not be reproducible. OBIA has been shown to be promising at mapping linear dune features (Vaz *et al.*, 2015) but scale is often disregarded within these methods so supervised classification is needed to ensure only features of interest are mapped. This becomes important when topographically small features are not differentiated from their larger/taller counterparts.

2.4.1 The crest mapping approach

Recently a script was introduced by Stepinski and Jasiewicz (2011) within the GrassGIS software (GRASS Development Team, 2015) package called *r.geomorphons* which uses Local Ternary Patterns (LTP) without a fixed window size (although a minimum search distance used to fine-tune the analysis). This method utilises pattern recognition using elevation values from DEMs rather than differential geometry to locate and map landforms and, as a result, is independent of scale (Jasiewicz and Stepinski, 2013). This is a significant jump forward for the modelling of coastal dunefields where the wavelength between dunes is highly variable and dunes are non-linear. It also offers a new automated and objective method to classify terrain features. Under this method, each cell of the DEM has its relationship to the eight cells around it analysed much like a flow direction/watershed model. Each surrounding cell is noted as higher, lower or equal to the central cell as long as the difference is greater than a tuneable flatness threshold. This analysis, when simplified for the effects of rotation, results in the 10 most commonly found landforms/geomorphons being mapped (Figure 2). As this method examines the DEM at a local scale and only requires each cell to be examined once, it is also very computationally efficient (Jasiewicz and Stepinski, 2013). However, it is important to note that any analysis based upon elevation models needs a bare-earth model to provide an accurate output so as to remove the effects of vegetation.

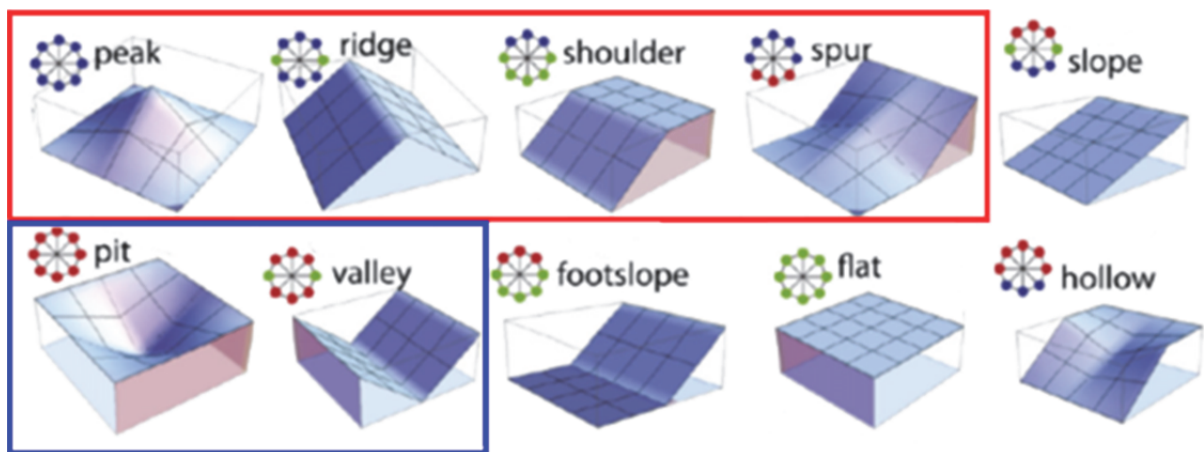


Figure 2: Ten most commonly found geomorphons (Local Ternary Patterns). The Geomorphons outlined in red are those that represent dune crest morphology (peaks, ridges, shoulders and spurs). Whilst those outlined in blue correspond to interdune locations (pits and valleys). Adapted from: Jasiewicz and Stepinski (2013), Figure 3 page 150.

One limitation of the script is that as it relies on raster DEMs and the geomorphons related to individual features are often more than one cell wide, as a result the creation of accurate crestlines is difficult and open to subjectivity by the user. A novel approach was needed to derive accurate, objective and reproducible polylines for the crest features. It was found that this process could be automated through the integration of flow direction based basin analysis within the ArcMap software (ESRI, 2014). This

method significantly limits the number of decisions needed from the user thereby resulting in less user subjectivity and consequently a crest map that is more reproducible. A simplified flowchart of the method employed within this study is shown in Figure 3.

During the preliminary parts of this study it was found that due to the high resolution and accuracy of the LiDAR-derived DEM, features that were less than 10 cm tall were detected and, there was a need for the DEM to be filtered so that only substantial dune features were modelled. This finding accords with similar studies (Stockdon *et al.*, 2009) that highlighted the need to filter LiDAR data to reliably extract dune crests. Consequently, an Adaptive Enhanced Lee (ALE) algorithm within ENVI was utilised (ENVI, 2015). For this study the Enhanced Lee filter was utilised as it has been designed to respond to both the relief and the noise level in a DEM thereby preserving features (Gallant, 2011). This differs from many other simpler filtering methods which assign an average value of a surrounding window regardless of noise level. The size of the filter used within any filter analysis can have a significant influence upon analyses performed (Gallant, 2011). Stockdon *et al.* (2009) suggested a filter window size of 20 m, however preliminary analyses of the filter outputs found that a more conservative 6x6 cell window was appropriate within this study (6-12 m window). Prior to running the ALE filtering on the DEM any regions with 'No Data' (e.g. where the DEM tiles did not overlap) was filled using the CON tool within ArcMap and a focal statistic of 3x3 circular mean. This method only fills the 'No Data' values within the study area using a mean value calculated from the surrounding nine cells and the process was repeated until all 'No Data' values within the DEM were filled. Following removal of the 'No Data' values, a series of transects was extracted across the filled areas to ensure minimal artefacts were present. The 3x3 circular mean was chosen due to the fact that dunes are highly topographically variable in space and therefore the use of localised cells was found to provide the most realistic output.

The azimuth of the maximum slope within 10 m of the slipface was derived using 10 m long perpendicular transects at 25 m intervals along the automated crestlines using the transect tool developed by Ferreira (2014). Points representing the locations of maximum slope were then derived using ArcMap Zonal Statistic Tool and aspect was then extracted from an aspect raster using the extract raster values to points (a flow diagram of this process and how heights were derived is shown in Appendix 2). A cut off of 10 m was used because of the close proximity and small size of some dunes.

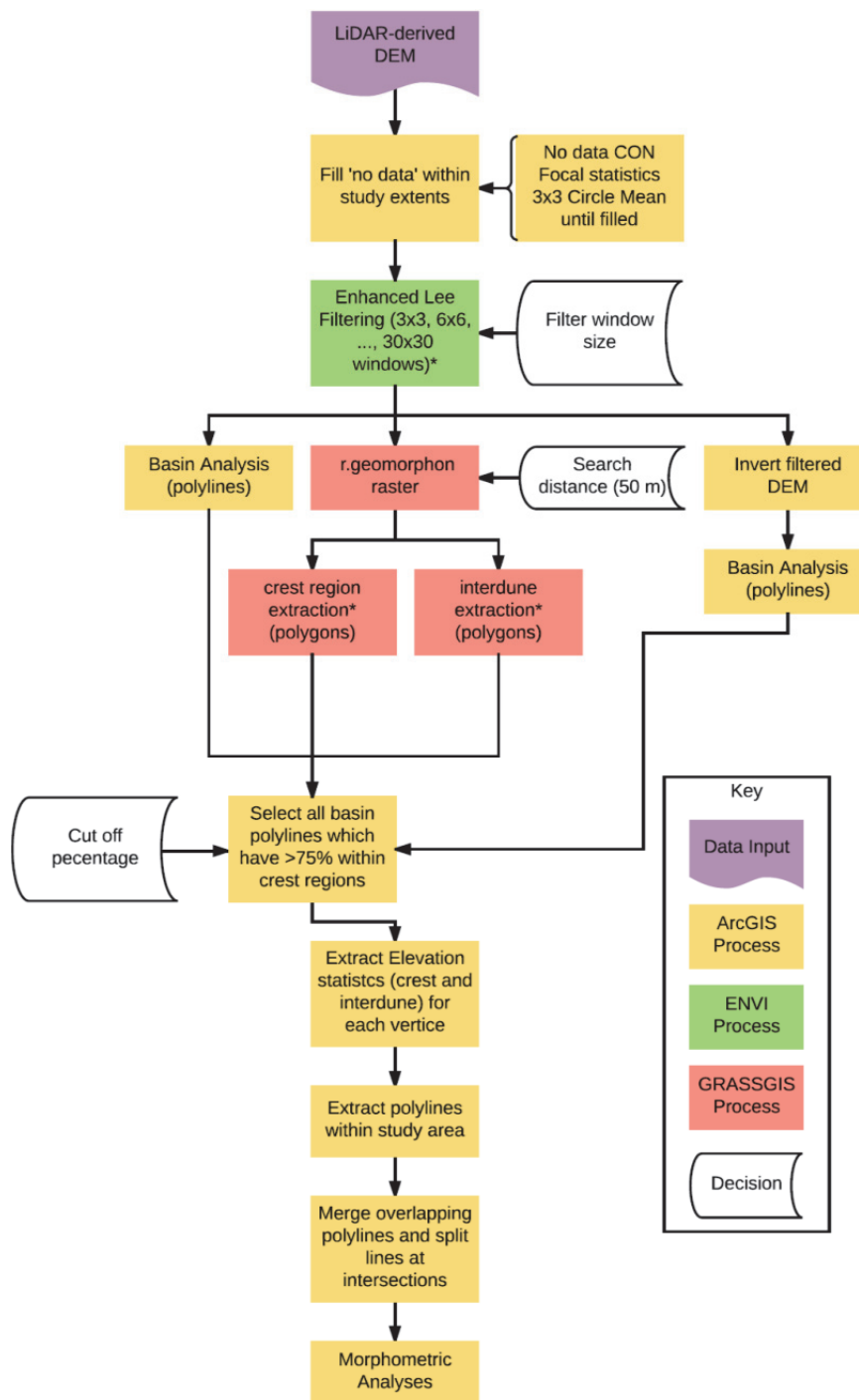


Figure 3: Simplified crest mapping model using LiDAR derived DEM. **Note:** This method was chosen as it is reproducible and largely removes user subjectivity. Three decisions are needed from the user to go from the raw DEM to the completed crestlines these include the **filter window size**, the **search distance** employed by the *r.geomorphon* script and the **cut off percentage** used to extract the crest polylines. *ArcMap CON tool used to select dune related 'crest' values 2,3,4,5 which were then converted to polygons within ArcMap.

2.4.2 Relative chronology and depth of the inter-dune surface

Investigations into the chronology of geomorphic and archaeological features have been increasingly aided by the use of portable Optically Stimulated Luminescence (pOSL) measurements as they prove to be relatively cheap and less labour intensive than tradition OSL analyses (Munyikwa *et al.*, 2012).

Luminescence profiling (Munyikwa *et al.*, 2012) can be successfully used to locate the base of dune sediment which otherwise can be hard to locate due to lack of variability of sediment texture with depth and between the dune and underlying sediment. Thom *et al.* (1992) primarily relied upon the degree of pedogenesis to separate Holocene and Pleistocene sand within SR because of the similarity of the particle size of the Holocene dune sands and underlying sediment.

Sample soil pits dug on a number of interdune surfaces were undertaken to help improve the accuracy of the volumetric analyses by the identifying the boundary between the Holocene dune and underlying sediment by pOSL photon counts and stratigraphy. The pits also allowed the examination of the degree of pedogenesis which helped inform a relative age sequence of each dunefield and enable comparisons of the soil development between the study dunefields (Bowman, 1989; Thom, 1987; Thom *et al.*, 1992; Thompson, 1981). All sample pits were located in the lowest part of each interdune surface where the Holocene dune sand overburden is thinnest (Fig. 4). Additional samples were also taken by augering within or beside the sample pit.

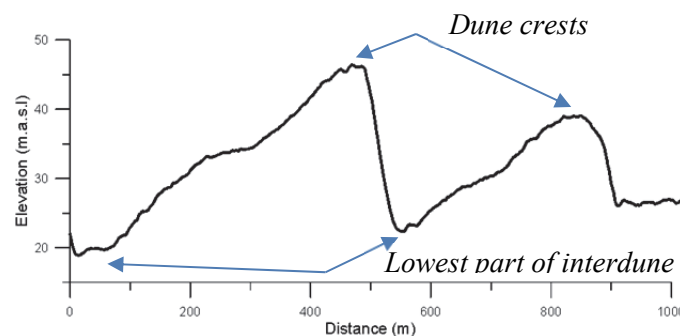


Figure 4: Pit locations in relation to dune crests/interdune locations.

Small (~2-3 cm) completely opaque sample vessels were pushed into the soil profile at regular intervals (~5-15 cm, dependent upon stratigraphic complexity). In dark room (red light) conditions, the bleached surface layer of each sample was removed and the remaining sample (c. 5-10 g) transferred onto a petri dish (5 x 2 cm [diameter x height]) covering the entire surface with a thin, levelled layer. Bulk sediment Infrared Stimulated Luminescence (IRSL) and Blue Light Stimulated Luminescence (BLSL) measurements of all samples were made using an upgraded SUERC portable OSL reader. Each sample was exposed to 60 seconds of infrared stimulation and then 60 seconds of blue light stimulation with any dark counts (luminescence during non-stimulation periods) subtracted from each measurement (Portenga and Bishop, 2016). The total photon count was normalised for dry sample mass by drying the samples in an oven at 80 °C for 24 hours.

The luminescence signal (photon counts) of a sample may be the result of the integration of the age of the buried sediment and their differing geological sources, the degree of pre-burial bleaching, and/or the degree of post-depositional disturbance (e.g. bioturbation) (Duller, 2008; Hanson *et al.*, 2015).

However when integrated with soil development and stratigraphy, it may offer insights concerning the relative age of the sample. When the pOSL samples suggested that the interdune/underlying sediment break was not reached, the depths gathered by the sample pits could be utilised as minimum depth values within the volumetric models applied.

2.4.3 Volumetric Analyses

The volumetric method used in this study relied upon interdune points created through the r.geomorphon analysis (see Figure 3) to locate the lowest parts of the interdune from which the boundary depths (if reached) were then subtracted. Points located on compound dune features were manually removed from the dataset and the ArcMap Topo to Raster tool was then utilised to create the before surface raster. A difference layer was then created using raster calculator and the expression:

$$\textit{Difference Raster} = \textit{LiDAR Derived DEM} - \textit{Presurface raster}$$

To estimate the inherent accuracy of the DEMs used within this study, sample points from overlapping DEMs within the NCB which should have experienced minimal change between the DEM acquisitions (in this case sealed roads) were digitised and their elevations extracted and then a regression analysis performed. It is important to note that these points represent the best case scenario concerning signal integrity and as such the assessment of error using this method should be assumed as such. To integrate the vertical inaccuracy inherent with the DEMs all volumetric analyses were run in ArcMap using the raster calculator tool and error bars shown on resultant figures. This accuracy measurement was undertaken on the filtered DEM used by this study not the raw DEM provided by the LPI. The DEM provided by the LPI has a stated vertical accuracy of 0.15 m and a horizontal accuracy of 0.6 m (NSW Department of Planning, 2008). Where the accuracy determined within this study was higher (i.e. error lower) than that stated by the LPI their more conservative accuracy was used.

2.4.4 Statistical Analysis of Dune Orientation

The multi-modular nature of dune orientation was analysed per dune group using a Newton-Fourier adapted Von Mises mixed model using movMF package in R (Hornik and Gruen, 2014; R Development Core Team, 2008)) with 10000 iterations and a 0.0001 convergence cut-off. This model was chosen due to its ability to analyse circular data and to detect an arbitrary number of modes. Von Mises mixture models have had a proven track record in the analysis of orientation based datasets such as wind and wildfire orientations (Barros *et al.*, 2012; Carta *et al.*, 2008; Masseran *et al.*, 2015; Masseran *et al.*, 2013). Von Mises models were run for integer modes between 2 and 6 with a 90% likelihood cut-off².

² When the log likelihood of the analysis reached 90 % of the log likelihood of the 6th group, this was used to select the model used for further analysis.

Coastal orientation was extracted using a linear direction mean (with ArcMap) from the national 100K Smartline (version 1) (Sharples *et al.*, 2009) coastline dataset clipped to the study coastline extent.

2.5 Results

2.5.1 Geomorphic Mapping

Seal Rocks

The SR dunefield shows the greatest spatial variability in dune form of all the study dunefields. As suggested by Thom *et al.* (1992) visual analysis of the dunefield does not suggest a series of dune generations but instead a complex of interconnected dune systems. To attempt to constrain morphometric and volumetric analyses within this study a series of dune groups were derived, moving from the most inland regions of the dunefield these include Bridge Hill, transverse dunes, unorganised network, inland parabolics, the foredune complex (further split into a coastal parabolic and beach ridges components).

Bridge Hill longwall trailing ridge

Bridge Hill is comprised of a highly sinuous crest made up of numerous linguoid lobes from advancing parabolic dunes forming a large compound precipitation ridge feature (which reaches up to 120 m.a.s.l. in close proximity to Seal Rocks road). The high resolution detail highlighted within this study supports the findings of Thom *et al.* (1992) but new features including many parabolic dunes which appear to wrap around the precipitation ridge along its entire length are now visible suggesting that these proximal parabolic dunes may have been reworked toward Bridge Hill and show how the trailing ridge may have formed and gained the linguoid morphology through the accretion of recurrent waves of parabolic and transverse ridges.

Transverse dunes

The transverse dune group is located in the landward edge of the dunefield in close proximity to Bridge Hill. Running at an oblique angle to the coastline, in the north they become more crenate and sub-parabolic and then ultimately transition into parabolic features. This suggests a temporal and/or spatial change in environmental conditions across the dunefield.

Parabolic dunes

Parabolic dunes are found mostly at the margins of the dunefield. These include those adjoining or forming part of the Bridge Hill ridge on the left-hand margin of the dunefield, those at the northern end of the transverse dunefield, those along the right-hand margin of the dunefield and smaller parabolics near the coastline. The informally named Mega Parabolic is a ~75 m tall compound parabolic dune feature found on the right-hand margin of the main SR dunefield. The dune is the largest member of the

inland parabolic dunefield group that extends to the northwest. From visual analysis of the DEM it appears that the Mega Parabolic is related to the presence of a north-south bedrock ridge.

Unorganised Network

The unorganised network dunes are located between the transverse dune group and the foredune complex. This region includes three main low lying sand sheets in the southeast which are largely devoid of dune features. These sand sheets were suggested by Thom *et al* (1992) to be deflationary surfaces that enabled significant volumes of sediment to pass through to the inland portions of the dunefield.

The Foredune Complex

Along the coast, parabolic dunes are commonly found downwind of areas of significant foredune instability and breakdown. The foredune complex includes these parabolic dunes, remnant beach ridges and vegetated nebkha.

Newcastle Bight

The extents of the various dune generations were adapted from the geomorphic and generational maps created by Thom *et al.* (1992) and adapted to the high-resolution LiDAR derived DEM. Three key Holocene generations were noted by Thom *et al.* (1992) including the currently active generation that has a protruding 'arm' extending to the southwest mid-way up the beach; a second generation wedged between the most seaward current generation and the most landward first generation. The first and second generations are no longer actively migrating and have been colonised by a diverse range of vegetation. The only exceptions are areas that have been cleared for sand mining operations. The current generation of dunes is largely devoid of vegetation and is actively migrating over the older second generation in the majority of the embayment and the beach ridge sequence in the northern and southern ends of the embayment. The actively migrating current generation of transverse dunes is separated by a sandsheet and deflation plain from the foredune.

Booderee

The Booderee dunefield comprises a series of beach ridges immediately behind the foredune in the southern end of the embayment and built in front of the rehabilitated foredune at the northern end. Landward of the rehabilitated foredune there are two generations of parabolic dunes. A small number of blowouts have formed from reworking of the rehabilitated foredune. An elevated sinuous ridge created from the accretion of parabolic dune heads within the northern 2/3rd of the Booderee dunefield marks the limit of the second generation of parabolic dunes.

2.5.2 LiDAR Accuracy

To estimate the inherent accuracy of the DEMs used within this study, sample points from the overlapping DEMs within the Port Stephens and Hunter DEMs which should have experienced minimal change between the DEM acquisition's (in this case sealed roads) were digitised and their elevations extracted and compared (Figure 5). The mean difference between the DEMs was 8.6 cm with a standard deviation of 8.2 cm. These values are within the range expected from the provider however this study will utilise their more conservative RMSE vertical accuracy ~15 cm provided by (NSW Department of Planning, 2008).

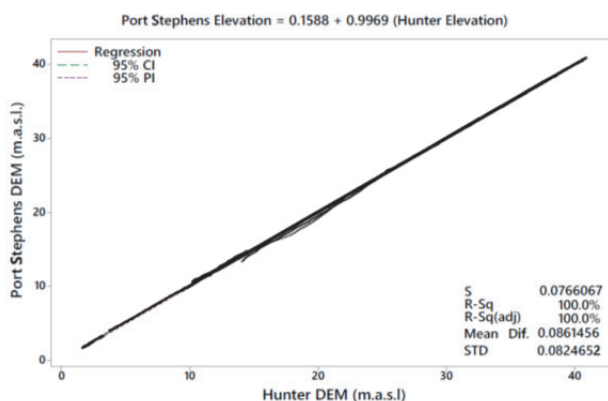


Figure 5: Regression analysis of vertical accuracy of LiDAR derived dataset within the NCB dunefield. Points were extracted from locations that experienced minimal change between LiDAR acquisition dates (i.e. sealed roads). Vertical accuracy noted concerns the final filtered dataset not the DEM provided by the LPI. Mean Dif. = Mean Difference STD= Standard deviation of mean difference.

2.5.3 Automated Crest mapping

The accuracy of automatically derived crests was assessed through the visual comparison of automated crestlines with manually derived crestlines within the SR dunefield and a series of topographic transects undertaken throughout the dunefields. During the early stages of this research, variations of the method were investigated. Basin lines with greater than or equal to a specified percentage overlapping the r.geomorphon-identified crest polygons were extracted into the final output which resulted in an improvement of accuracy. Visual analysis of the final product found that dunes with erosional surfaces (hollows) and poorly-defined crests were less clearly identified because they were modelled as valley slopes not crestlines. This was most apparent in the northern sections of the NCB current generation where a complex of crescentic, sub-parabolic and barchanoid dunes dominate (Figure 6 b). The approach performed well when modelling transverse, parabolic, beach ridges and compound features (Fig. 6 a,b,c,d).

A cut off value of crestlines with a height above the nearest interdune of ≥ 1 m was implemented to ensure that only substantial dune features were included in subsequent morphometric analyses. Due to the reliance upon ArcMap basin tool, all crestlines derived within this approach must represent locations that have no cells flowing into them and thus the detections of false positives should be minimal.

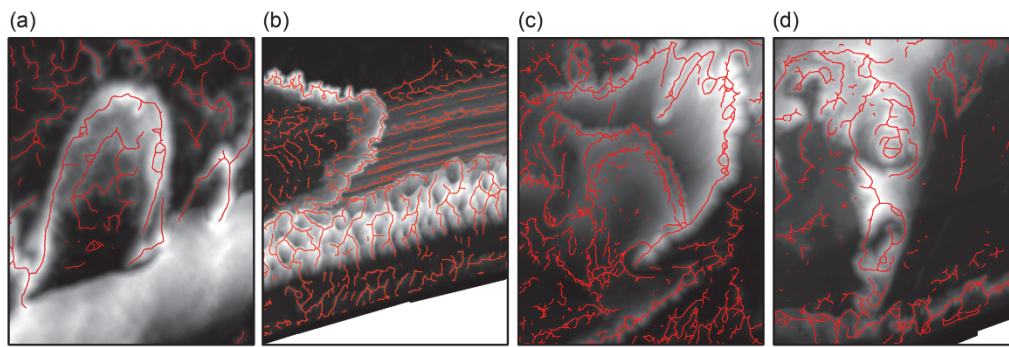


Figure 6: Examples of crestlines derived using automated approach: (a) parabolic dunes Booderee, (b) Beach ridge sequence and current and second generation dunes NCB, (c) 'Mega Parabolic' and Treachery Head Parabola SR, (d) complex dune feature SR.

2.5.4 Dune Orientation: azimuth of maximum slope (within 10 m of dune crest)

Seal Rocks

Foredune Complex (Parabolics and Beach Ridges)

The orientations evident in the rose plots of Figure 8 show three main modes of orientation. The dominant modes to the southeast (36.9% of orientation points) and northwest (51.4%) represent the parabolic dunes within the foredune complex. The remaining sub dominant south-south-eastern mode (11.7%), normal to the coast, represent the beach ridges.

Transverse dunes

There is a large scatter in the azimuth of maximum slope detected within the transverse dune features (Figure 8). When two modes are considered the azimuth of maximum slope is almost parallel to the coast, with a north-easterly (249°, 42.8%) and south-easterly (75°, 57.2%) direction suggesting a dominant crest orientation almost perpendicular to the coast (162° - 342°) which is supported from visual analysis of the DEM.

On closer examination of the transverse crestlines it is evident that the significant scatter seen within the slipface azimuth is likely due to the increasingly crenate and linguiodal nature of the crests. Other potential factors which could partially account for this scatter include the presence of ~30 reversed transverse dunes spread throughout the transverse dune group (evident in Fig. 8).

Parabolic Dunes

Throughout the dunefield there was no major deviation in parabolic dune orientation (Fig. 7) between those dunes found along the coast within the foredune complex, which had dominant modes towards the southeast (113° representing 47.5 % of points) and northwest (300° with 52.5%) to those found in the inland region of the dunefield which had dominant orientations towards the southeast (107°, 54%) and northwest (291°, 46%). Inferred orientations of the dunes (bisector of the two dominant

orientations) deviated by less than 10° between the coastal generation (26°) and the inland parabolics (19°).

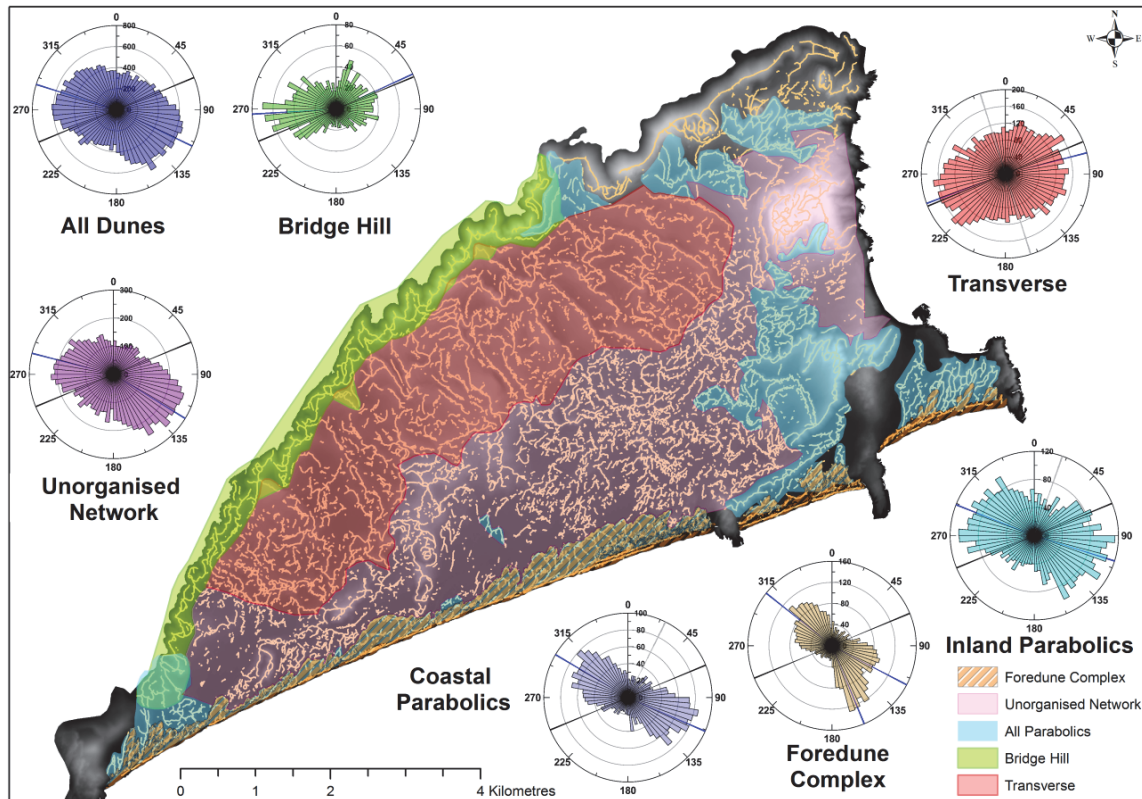


Figure 7: Dune azimuth of maximum slope (within 10 m of modelled crestline), a measure of slip face orientation within the Seal Rocks. **Note:** the black rose plots represent the linear directional mean of the upwind source coastline, the dark blue rose plot represents the major modes extracted by the Von Mises statistical analysis and the grey rose plot represents the orientation of the parabolic head (based on angle bisection as suggested by Jennings (1957)) or the inferred dominant crest orientation inferred from the orientation rose plot. See Appendix 3 for other modelled mode group directions.

Unorganised Network

Analysis of the orientation of this complex (Fig. 7) shows dominant slip face orientations to the north-west and south-east. This region is comprised of a mixture of relatively unorganised transverse dunes with regions of significant reworking visible forming crenate ridgelines. A minor constituent of this group is several annular features which range from < 100 m to ~1.5 km long and may represent a complex deposition of sand around fixed obstructions. Overall, this dune group highlights the geomorphological complexity revealed by the high resolution of the DEM but shares the dominant modes and variability seen within the inland parabolic group.

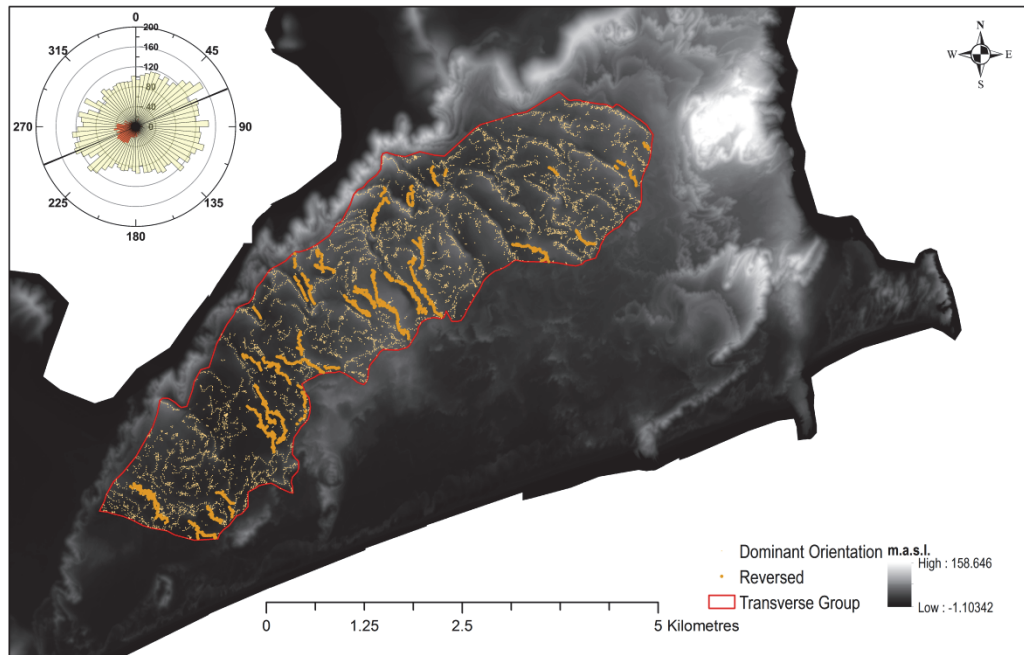


Figure 8: Location and orientation of reversed transverse dunes within Seal Rocks dunefield. **Note:** the negligible contribution of the south western orientation provided by reversed dunes.

Newcastle Bight

Current Generation

The dunes within the current generation have slip faces aligned at ~40 degrees oblique to the coastline, with an almost equal distribution between the ESE (52.6%) and WNW (47.4%) (Fig. 9). Within the southern current generation this relationship is altered so that there is a slight dominance of the ESE (55.6%) over the WNW (44.4 %) and a shift slightly to the south in both components as compared with the north.

Beach ridge sequence

The beach ridge slope azimuths are orientated nearly normal to the coastline but with a slight dominance of 56.5% of the values being partitioned into the landward mode whilst 43.5% to the coastal when two modes are modelled (Fig. 9).

When four groups are modelled (not shown) the two additional modes detected appear to represent the variation in coastal orientation between the south and northern ends of the compartment with a similar proportion of points (57.5%) being represented by the landward facing modes.

Second Generation

When two modes are modelled within the second generation a subdominant mode is found to the east south east (107°, 39.9% of points) and a dominant mode to west south west (250°, 60.1%).

First Generation

The first generation dunes show greater variability in orientation than the other dune groups with 4 modes modelled to achieve the 90% cut-off. There are two slightly dominant modes to the SSE (27%) and west (32.8%) with two minor modes to the north (20.7%) and east (19.5%).

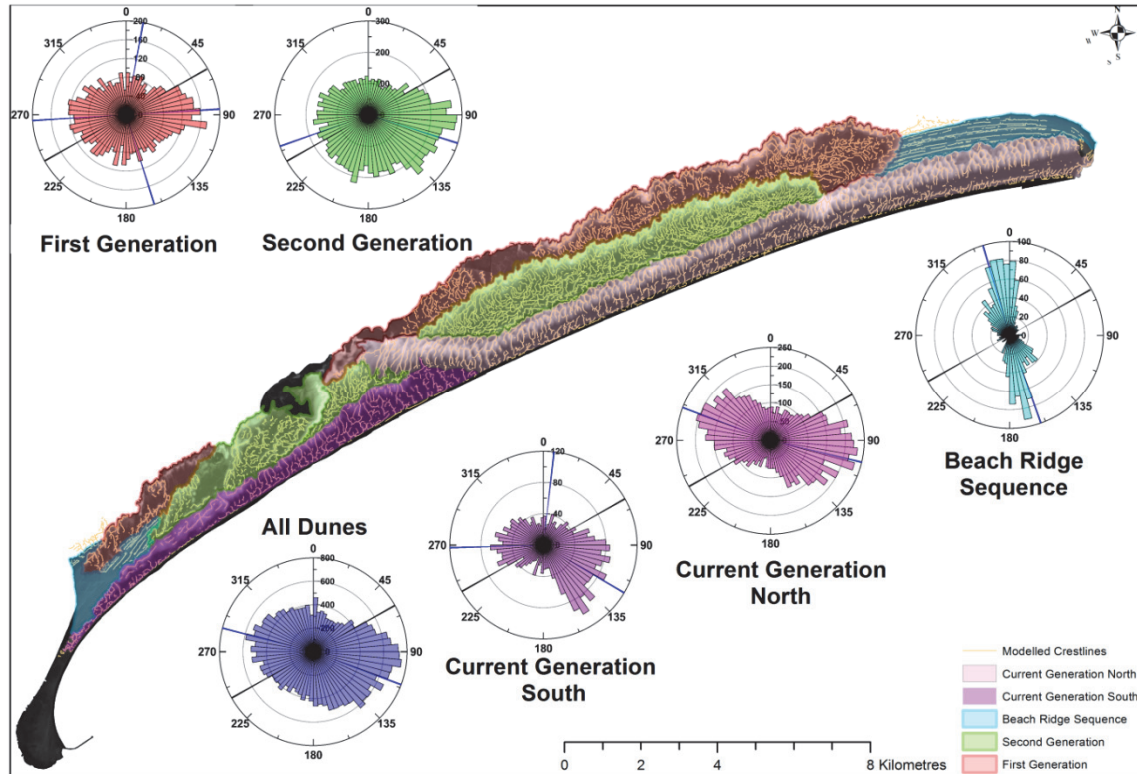


Figure 9: Dune azimuth of maximum slope (within 10 m of modelled crestline), a measure of slip face orientation within the NCB. **Note:** the black rose plots represent the linear directional mean of the upwind source coastline, the dark blue rose plot represents the major modes extracted by the Von Mises statistical analysis.

Booderee

Beach ridge sequence

The beach ridge slope azimuths are orientated nearly normal to the coastline but with an almost equal number steepest towards the coast (50.2%) to that away from the coast (49.8%) (Fig. 10). There is a small but obvious difference between the two modal directions, slightly obtuse to the coastline, and the two modelled means.

When four groups are modelled (not shown) the two additional modes detected appear to represent the variation in coastal orientation between the south and northern ends of the compartment with a similar proportion of points (50.4%) being represented by the coastward facing modes.

First and second generation parabolics

There does not appear to be significant variation of the parabolic dune orientation between the two generations. There is a very large variability of slope azimuths with a weak east-west bimodality. There are subtle difference between the two generations (the two modes vary by < 10 degrees between the

two generations) evident in Figure 10, including a slight dominance of southward (shoreward) sloping dunes over northward (inland) facing dunes in the first generation dunes.

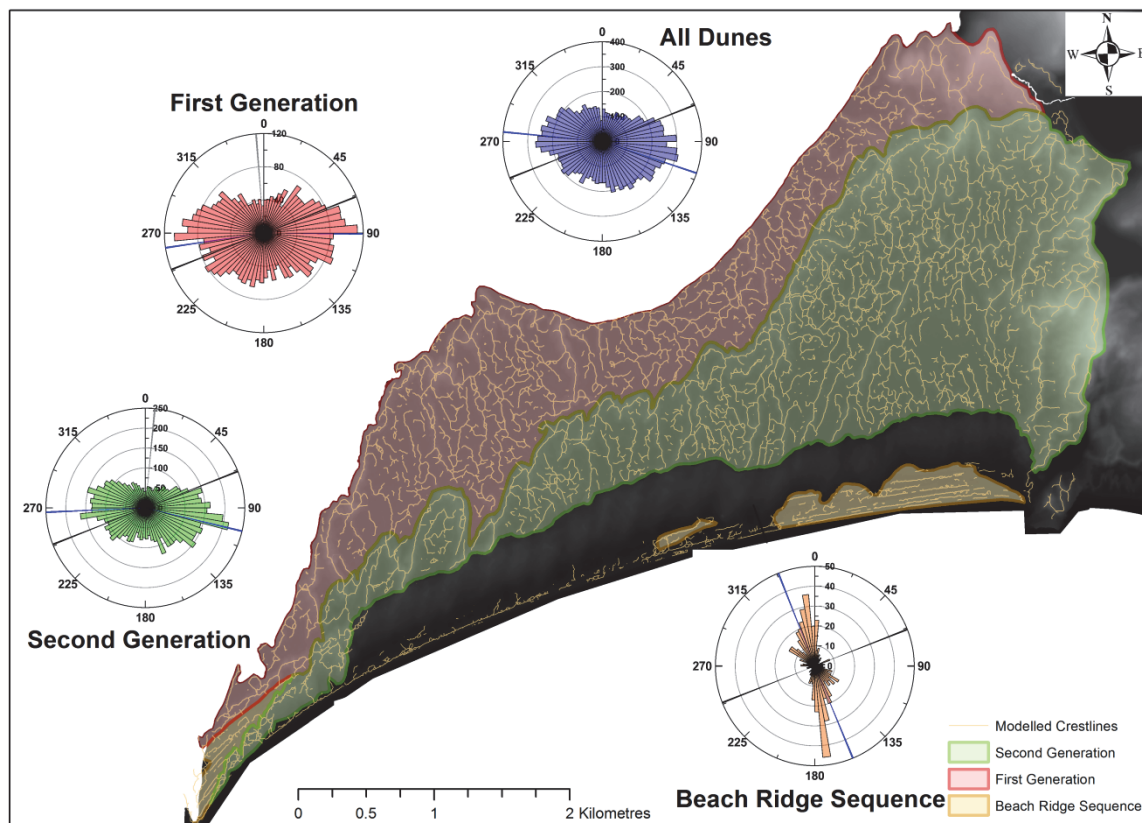


Figure 10: Dune azimuth of maximum slope (within 10 m of modelled crestline), a measure of slip face orientation for (a) Booderee, **Note:** the black rose plots represent the linear directional mean of the upwind source coastline, the dark blue rose plot represents the major modes extracted by the Von Mises statistical analysis and the grey rose plot represents the orientation of the parabolic head (based on angle bisection as suggested by Jennings (1957)) or the inferred dominant crest orientation inferred from the orientation rose plot. See Appendix 3 for other modelled mode group directions.

2.5.5 Dune Height

The dune height analysed within this study is that from the crest height to the nearest interdune. This measure of dune height is likely an underestimate of the height of complex/compound dunes where the nearest interdune resides upon that feature. However this measure ensures that the measured heights are both replicable and objective in nature. A one metre cut-off value was utilised to ensure that only substantial dune features were included within the analysis. Within the beach ridge sequences it is interesting to note that the NCB ridge sequences appear to be taller and have larger height variability than the Booderee beach ridges (Fig. 11). This may be due to differences in sample size and/or differences in sand supply. The beach ridge sequences are the lowest dunes and have the least variability in height of all the dune groups analysed whilst Bridge Hill longwall trailing arm and the inland parabolics within SR had the greatest height and height variability.

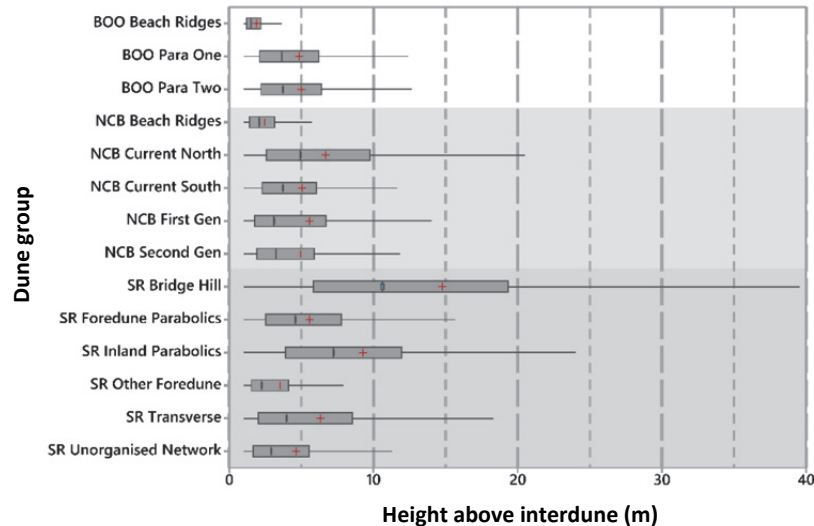


Figure 11: Box plot of major dune groups within Booderee (BOO), Newcastle Bight (NCB) and Seal Rocks (SR) dunefields. See Appendix 4 for table of raw values.

2.5.6 Portable OSL and degree of pedogenesis

Pedogenesis within all pits within SR showed a podzol formation, with the exception of Epsilon pit that showed evidence of complex interactions with the water table (Fig. 12). Most profiles showed unexpected variations in photon counts with depth. Most profiles showed an association between soil horizons and OSL counts. Within Gamma, Beta and Alpha pits both IRSL and BLSL increased significantly within the A2 horizon. There was a complicated and highly variable relationship within B2s, B2sh and B2h horizons. Within Alpha, B2s saw an increase for the first metre and then plateaued; within Beta, B2sh was relatively stable until ~175 cm before decreasing significantly; at Gamma there was a general decrease in the B2h and increase in B2s; Delta saw a general decrease in B2h, increase in B2sh and decrease in B2s. Within Epsilon pit there was a significant increase in both IRSL and BLSL with depth to ~125 cm within the dark brown to strong yellow horizons before largely plateauing off for the remainder of the profile. Within the Transverse pit there was a general increase in BLSL with depth whilst IRSL remained highly variable and at times below the detection threshold.

All sites within the NCB except SA hit the water table within the pit (< 1.5 m below the surface) (Fig. 13). Therefore, the analysis of degrees of pedogenesis was significantly restricted. It is evident that within the A2 horizon both the IRSL and BLSL values increased significantly from those of the A1 horizon before plateauing and generally decreasing with depth.

The depth of the A2 horizon is significantly deeper within the northern SA and mid-embayment SD profiles where the water table was deeper.

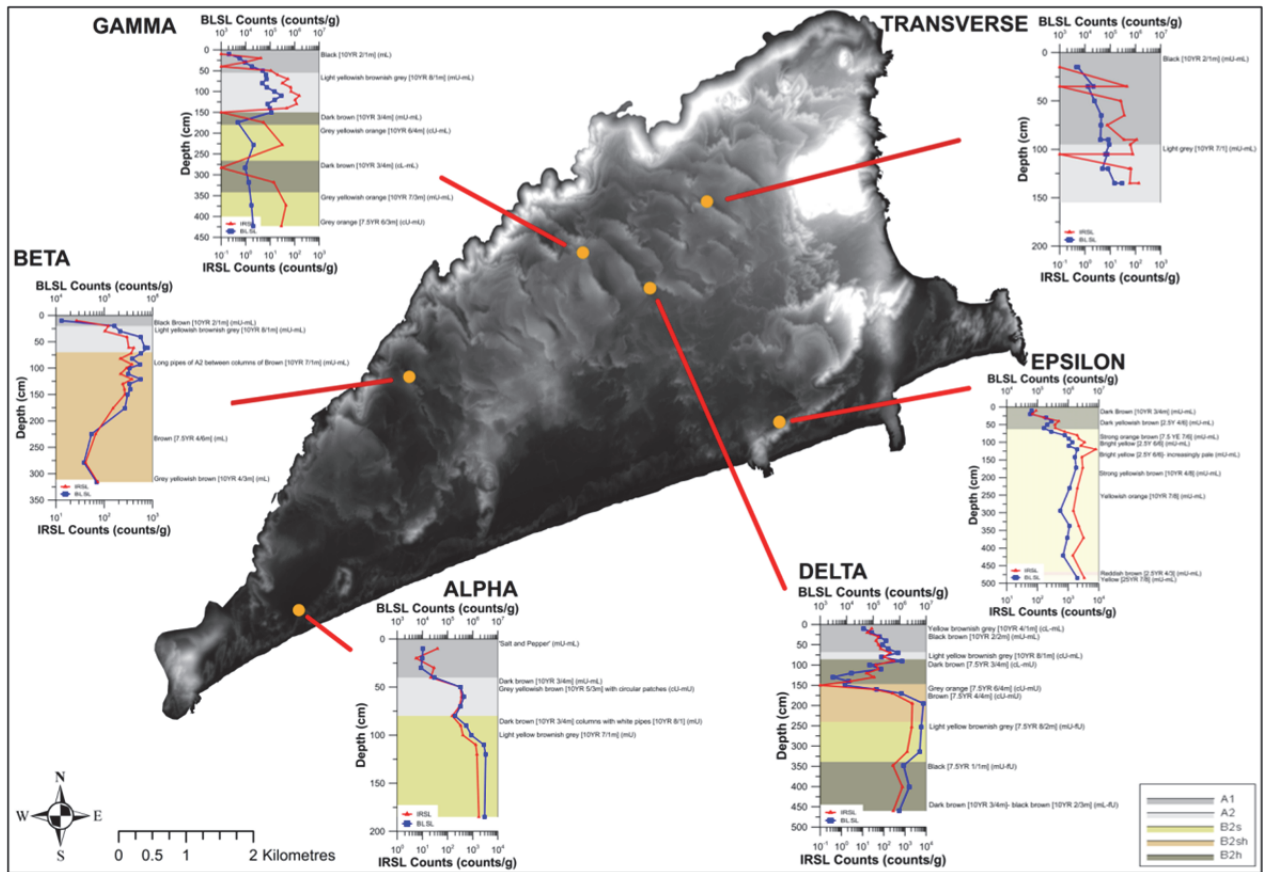


Figure 12: Soil sample pit locations within the SR dunefield including inset pOSL and sediment profiles.

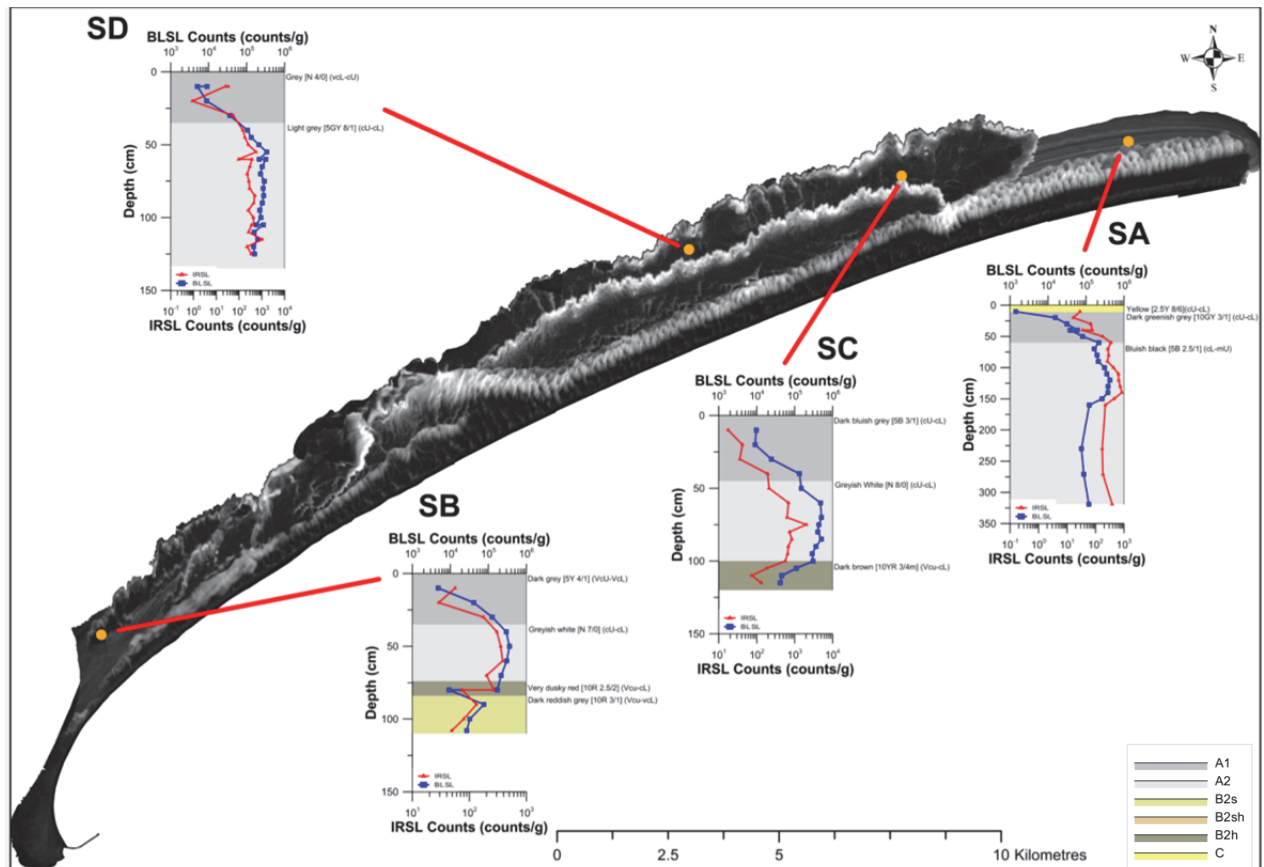


Figure 13: Soil sample pit locations within the NCB dunefield including inset pOSL and sediment profiles.

2.5.7 Area-normalised volumes per dune group

Normalised (km^3/km^2) volumes per dune group

Figure 14 shows the area normalised (km^3/km^2) volume of each dune groups within each of the study dunefields. SR (Fig. 14 a) has significantly higher normalised volumes than both the other sites. The NCB (Fig. 14 b) and Booderee (Fig. 14 c) have similar normalised volumes. Bridge Hill in the SR dunefield stands out as a dune group with significantly above average normalised volumes, accounting for 35.7% of SR total dunefield volume.

There is a noticeable difference within the current generation group between north and south NCB (Fig. 14 b). It is evident that the beach ridge sequences within Booderee and NCB provide a relatively small percentage of their constituent dunefield volumes. There is a noticeable difference between the normalised volume of the beach ridges seen within Booderee ($2.73 \text{ km}^3/\text{km}^2$) and NCB ($6.04 \text{ km}^3/\text{km}^2$).

Overall normalised dunefield volumes within Booderee $6.82 \text{ km}^3/\text{km}^2$ and NCB $7.25 \text{ km}^3/\text{km}^2$ pale in contrast to SR with $12.73 \text{ km}^3/\text{km}^2$.

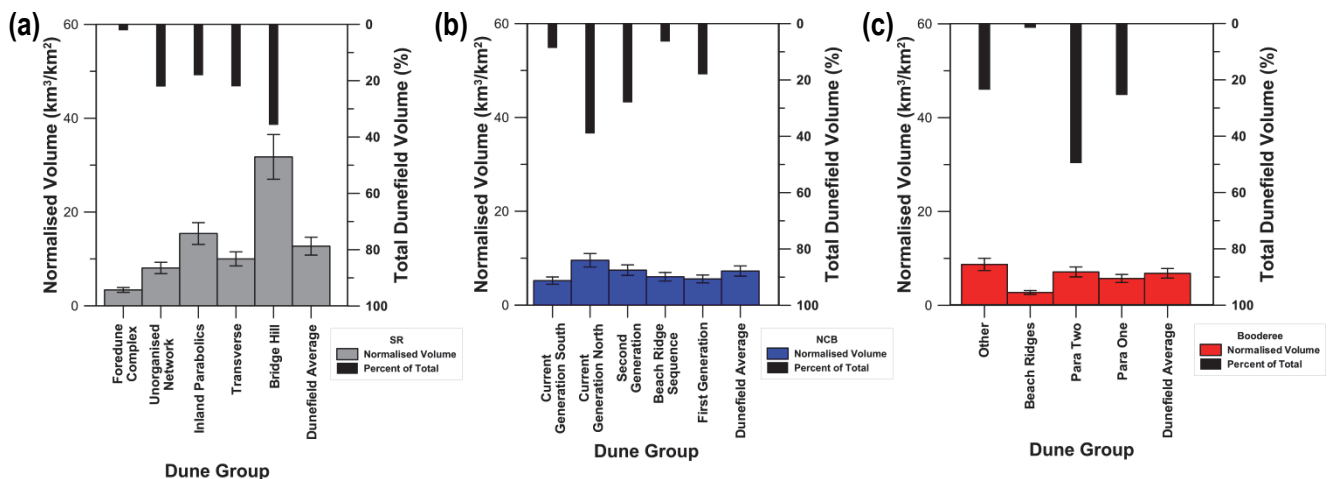


Figure 14: Normalised dune volumes per km^2 within (a) Seal Rocks, (b) Newcastle Bight, and (c) Booderee dunefield. Note: dune volumes have been normalised to 1km^2 areas to ensure values can be compared within and between study sites. The values shown on the top of each column is the volume percentage (%) of the total dunefield volume. See Appendix 5 for volumes table.

Change in volume with distance from current coastline

There is a general increase in volume with increased distance from the coast within all study sites (Fig. 15); with the exception of NCB where the normalised volumes within the current generation outweigh those found within the first and second generations combined.

SR dunefield (Figure 15 a) has migrated further inland than the NCB (Figure 15 b) and Booderee dunefields (Figure 15 c) despite, or because the dunefield being confined by several bedrock outcrops. The NCB dunefield has migrated the least inland despite currently showing the greatest activity and having the least confinement of all the study dunefields evident through the lack of bedrock

confinement and/or topographic relief inland of the dunefield. There was an observed increase in both barrier width and volume from the southern to the northern current generation within the NCB (Fig. 15 b).

Within the SR dunefield the significant increase in normalised volume seen in the inland parabolics group at ~2700 m to ~3200 m inland is primarily due to the influence of the uncharacteristically large 'Mega Parabolic' feature.

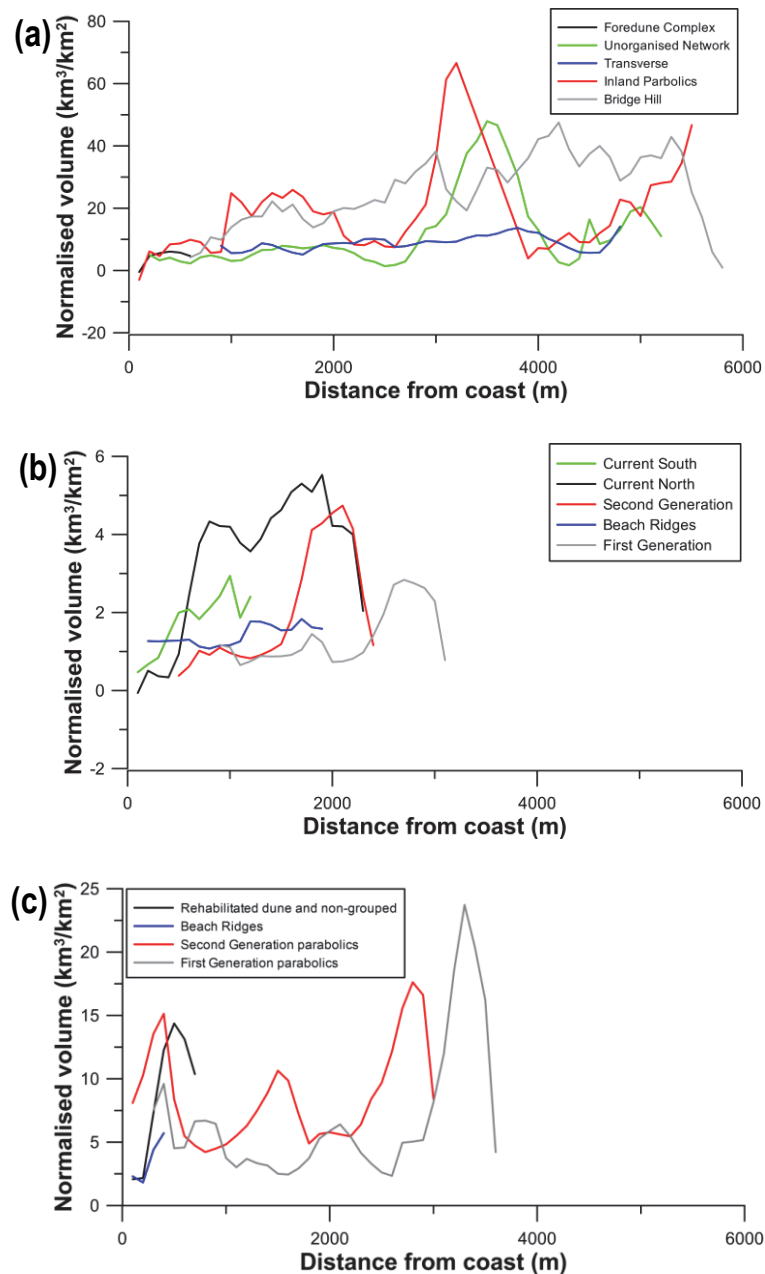


Figure 15: Normalised volume (km^3/km^2) within each dunefield group with increasing distance from current coastline (based on 100 m intervals). (a) Seal Rocks, (b) NCB and (c) Booderee dunefields. **Note:** The volumetric analyses of SR includes the mined section of Bridge Hill and the altered section of the unorganised network immediately coastward of the mined area.

2.5.8 Embayment slope

Figure 16 shows perpendicular transects taken from the midpoint of the study coast into each study embayment, based on the Australian bathymetry and Topography dataset 2009 (Whiteway, 2009). This figure provides a rough estimate/proxy of sediment supply to the study dunefields assuming that the continental shelf has a plentiful supply of sediment. Studies have linked the bathymetry of embayments to the size/sediment supply to their dunefields (Short and Hesp, 1982). All the study embayments have a steep slope proximal to the beach and, as a result, wave energy is relatively high. The SR embayment has the steepest slopes of the study embayments. The Bherwerre Beach of the Booderee embayment has an intermediate gradient followed by Stockton Beach (NCB) within the greatest distance to 60 m.b.s.l. The sediment area available to each beach can be estimated by the inverse relationship with gradient i.e. the greater the distance to 60 m.b.s.l. the greater the area that is available for sediment mobilisation. Stockton and Bherwerre beach have the highest area available for sediment mobilisation followed by Submarine, Treachery and Lighthouse Beach. This relationship only takes into account a single 2-D representation of the embayment. Other factors such as longshore drift and total embayment size also contribute to sediment supply.

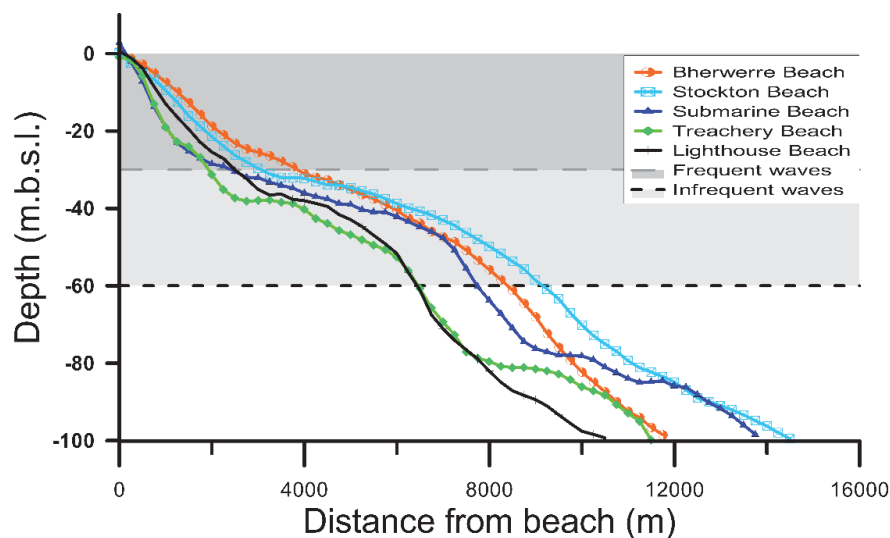


Figure 16: Embayment slope from midpoint of study beaches to 60 metres below sea level (m.b.s.l.). The shaded grey and light grey regions denote the depths of sand mobilisation on the southeastern Australia continental shelf for frequent waves and infrequent estimated by Griffin et al. (2008).

2.6 Discussion

2.6.1. Late Holocene sediment supply

The pOSL profiling undertaken as part of this study revealed complex patterns which did not conform to the expected pattern of increasing luminescence signal with depth (Figure 12 and 13). Possible causes include the incomplete bleaching prior to last burial, varying degrees of bioturbation, variable dose rate (due to presence of heavy minerals within the profile) (Roy, 1999) and groundwater interactions. In

some profiles it is likely that we did not reach deep enough to reach the interface between the interdune and underlying Pleistocene sediments. No sites experienced the characteristic 'hockey stick' change in photon count shown to occur within the dune and underlying sediment interface (Munyikwa *et al.* (2012). The only sites in which an interval of significant accumulation was reached (denoted by the plateauing of the BLSL and/or IRSL counts representing rapid accretion) was within Alpha, Delta and Epsilon pits at SR. However Alpha pit was the only profile that did not show noticeable variability with increasing depth within this plateau region. As a result of these findings, and to improve consistency between the sites (as no pits were undertaken within the Booderee dunefield), volumetric analyses were based upon a pre-surface constructed from interdune elevations derived using the automatic crest mapping method on an inversed DEM.

Results of the volume analysis show that SR had the highest dunefield volume and normalised volumes of all the study sites. This most likely arises from the greater sand supply within the SR embayment due to the presence of confining bedrock outcrops (Thom *et al.*, 1992) and greater longshore compartment length, which resulted in an enhancement of both dune height and volume. SR had 1.3 times the total estimated volume of the NCB suggesting an enhanced sediment supply during the HMT (see Appendix 5). Most of the sediment was found to be within the inland regions of the dunefield suggesting a surge of sediment supplied to the system during the late Holocene with major dune construction between 3025 ± 135 yr B.P through to at least 1265 ± 135 yr B.P before being stabilised quickly by vegetation (Thom *et al.*, 1992). The diminutive volume found within the current foredune complex suggests a significant decrease in sediment supply since stabilisation. Fluctuations in sand supply are also indicated by the low-relief deflation plain between the foredune complex and inland transverse and parabolic fields. Due to the triangular shape of the dunefield and its extension to the northeast Figure 15 (a) shows an increase in sediment stored in the inland and especially northwestern parts of the dunefield. This suggests significant downwind movement of sand (to the northwest) during the late Holocene before a reduction in sand supply resulted in a decrease in dune volume and height in the southeast. This is especially evident within Bridge Hill which increased in volume with increased distance inland. Similarly the inland parabolic group shows two major peaks in volume one at 2700 - 3200 m inland which represents the location of the 'Mega Parabolic' and another one at 4600 - 5500 m inland representing the parabolics in the far northwestern section of the dunefield in close proximity to Bridge Hill. These regions show the increased migration of sediment to the far upwind locations of the dunefield. Compared with the significantly lower normalised volumes of the unorganised network (< 2000 m inland) and transverse dunes, this suggests a significant decrease in sand supply within the younger coastal sections of the dunefield which is also supported by the presence of the deflation

plains. The presence of the unorganised network group likely suggests a transition period where sediment supply started to decrease.

The transition from transverse to more parabolic forms in the far northwest suggests a decrease in sediment supply or a more likely an increase in stabilisation by vegetation as is suggested by the change in normalised volume.

The Booderee dunefield shows signs of an increased sediment supply over the late Holocene. The younger Booderee second generation parabolics, beach ridges and other dunes (primarily comprised of the rehabilitated foredune) represent ~75% of the total dunefield volume. However, it is likely that a significant proportion of the first generation parabolics within the dunefield has migrated into St Georges Basin and then been reworked by wave action into sand bars. As such this volumetric analysis should likely be taken as an under estimate of the volume of the first generation of dunes. The presence of the two phases of parabolic dune formation suggests that the sediment was likely delivered in a series of pulses instead of a steady increase in supply.

The NCB has shown sediment supply to increase significantly over time since its first generation formation, with just over half of the sediment within the system being stored within the current generation of dunes. This apparent increase in sediment supplied to the system during the late Holocene supports the findings of Oliver *et al.* (2015) and Goodwin *et al.* (2006) elsewhere on the NSW coast. However the presence of the inter-barrier sandsheets between the current and second generation, and second generation and first generation barriers suggests either a decrease in sediment supply between the major phases of barrier construction and/or that these sandsheets acted as regions of enhanced transport during the late Holocene.

Within the Booderee dunefield it has been shown that there may have been a slight change in dominant wind direction (<10 degrees) between the first and second generation of parabolic dune formation thereby supporting the idea that the dunefield activated in at least two generations. Within the SR dunefield minimal difference between the orientation of coastal and inland parabolic dune features suggests that the entire dunefield formed under the same wind regime in a single phase largely supporting the findings of Thom *et al.* (1992). The lack of major orientation changes within the various parabolic dune and transverse dune generations within all the study sites suggests either wind direction has not changed substantially or that the broad scatter of dune orientations prevents detection of relatively minor changes in wind direction. It is possible that variations in swell and wave direction contributed to the changes in sediment supply to these dunefield but are not detectable within the dunes themselves.

2.6.2 Dune morphology and sand supply

It is evident from Figure 15 (a) that the majority of dunefield volume within each of the study dunefields is comprised of transgressive dunes with morphologies suggesting various degrees of activity (i.e. parabolic and transverse dunes). The absence of major regions (both spatially and volumetrically) of beach ridges suggests that increased sediment supply and varying degrees of stabilisation by vegetation have resulted in beach ridges being reworked into parabolic and transverse dune features and/or that there was a continuous supply from the back beach (Hesp, 2013). This inequity in dune form is evident in the beach ridges within the NCB which only account for 6.38% of the total volume of the NCB dunefield and are actively being migrated over by the current generation within the northern and southern extremes of the embayment. Similarly within the Booderee embayment the beach ridges account for 1.51% of the total dunefield volume with the rest of the dunefield comprised of parabolic dune features. Within the SR embayment this is exemplified by the fact that the foredune complex which is comprised of beach ridges and parabolic dune features only accounts for 3.88% of the total dunefield volume. It is evident in Figure 11 that the beach ridge groups have the lowest height variability and mean heights of all the dune groups. This is likely due to the fact that any aeolian capping is based upon non-dominant onshore winds (Figs. 8-10) as compared to the parabolic and transverse dunes that have slip face orientations showing evidence of sand movement by the dominant south easterly winds.

2.6.3 Automated dune crest mapping

The derived crestlines shown in Figure 6 highlights that the approach accurately identified dune crests within the study site used in this research. The deriving of crestlines allowed quantitative analysis of dune orientation largely free of user-based subjectivity and revealed unexpected patterns in the orientation of different dune types.

The problem concerning the continuity of crestlines due to the misidentification of crests as valley slopes remains an important avenue for future improvements in the method.

2.7 Conclusions

The analysis of LiDAR derived DEMs through the use of a novel crest mapping approach has enabled an unparalleled glimpse into the long-term (Holocene) evolution of these dunefields. It has highlighted the high degree of complexity of dune form and evolution found within these systems; showing diverse range of dune forms in close proximity to each other.

This study has also highlighted the need for strategic OSL dating to help constrain the temporal resolution and improve the accuracy of models concerning the formation and evolution of these coastal

dunefields. These dunefields show different sediment supply regimes during the late Holocene with SR supporting the decrease in sediment supply suggested by earlier studies (Davies, 1986, Short, 1988, Short and Hesp, 1982). In contrast the Booderee dunefield shows the potential of increased sediment supply over the late Holocene and NCB strongly suggests an increase in supply supporting the findings of Oliver *et al.* (2015) and Goodwin *et al.* (2006).

Further analysis of the crestlines derived in this study show promise to offer invaluable insights into how these dunefields evolved especially when integrated with stratigraphic dating.

2.8 Acknowledgements

This research was funded by a Macquarie University postgraduate research fund (Farebrother). We would like to thank the NPWS and Worimi Conservation Lands for permitting access and permission to excavate within the National Park. A special thanks to the NSW LPI for providing the LiDAR-derived DEMs.

2.9 References

Combined reference list can be found in Chapter 5.

Chapter 3: Short-term migration of southern Newcastle Bight dunefield detected by multi-temporal LiDAR

Purpose: This chapter presents original research that has been entirely undertaken within this MRES year (January 2016-October 2016). The chapter provides a journal paper draft including an Abstract, Introduction, methods and an integrated results and discussion related to the short-term evolution of Southern NCB dunefield and compares it to other studies undertaken within the study area. This chapter will cover aim (iii). There has been no high resolution analysis of short-term dunefield morphology of the NCB or dunefields within Australia and as such this research will help underpin future research and management of this system.

Format: In accordance with the Macquarie University policy for higher degree research thesis by publication³ this chapter has been written for submission to a peer-reviewed journal. Repetition and any referencing and stylistic inconsistencies have been minimised to facilitate the thesis examination process. Supplementary material and references referred to in the paper are provided in the reference list and appendices at the end of the thesis, and are intended to become the references and supplementary material provided in the published version of this paper.

Author contributions:

William Farebrother: conducted GIS analyses, analysed all the data, designed all figures and tables, wrote and edited the paper.

Paul Hesse: helped develop the study and provided an excel spreadsheet to calculate DP, RDD and RDP from AWS data, provided help editing the paper and supervised W.F. in the research undertaken.

Abstract:

Studies have highlighted the need to understand how coastal dunefields migrate over time, to inform their future management. This study uses volumetric analyses of multi-temporal LiDAR and a novel automated dune crest mapping approach to reach this understanding. Results suggest that short-term dune migration (2007-2013) within the southern Newcastle Bight is dominated by the SW-NE oriented dunes moving towards NW, and the NW-SE oriented dunes towards the NE. Sand movement within the northern end of the study area was found to be greater than in the south. These patterns follow the

³ The Macquarie University policy for thesis by publication states that a thesis may include a relevant paper or papers that have been published, accepted, submitted or prepared for publication for which at least half of the research has been undertaken during enrolment. The papers should form a coherent and integrated body of work. The papers are one part of the thesis, rather than a separate component (or appendix) and may be single author or co-authored. The candidate must specify their contribution and the contribution of others to the preparation of the thesis or to individual parts of the thesis in relevant footnotes/endnotes. Where a paper has multiple authors, the candidate would usually be the principal author and evidence of this should appear in the appropriate manner for the discipline. MQ Policy: http://www.mq.edu.au/policy/docs/hdr_thesis/policy.html

seasonal pattern of onshore and offshore winds and result in the simultaneous longshore movement and landward transgression of the coastal dunes.

3.1 Introduction

Airborne Light Detection and Ranging (LiDAR) has successfully been used internationally to explore the short-term migration and longer term evolution of coastal dunefields (Hugenholtz *et al.*, 2012; Levin *et al.*, 2014; Mitsova *et al.*, 2004; Woolard and Colby, 2002; Zhou and Xie, 2009). It has been shown to offer unparalleled high resolution glimpses into the morphology of dunefields resulting in the ability to understand the structure and short-term migration of these systems like never before. Multi-temporal LiDAR DEMs can provide a more accurate estimation of dune migration than analysis of aerial photographs due to the significant increase in resolution and locational accuracy of the dataset. It also enables the ability to derive accurate estimations in volumetric change for an entire area rather than selected transects undertaken during fieldwork.

LiDAR surveys along the Australian coast have previously been infrequent and sparsely distributed. Thus, studies into the short-term evolution of coastal dunes in Australia have relied upon costly repeated site surveys, and have consequently been relatively rare. The Newcastle Bight (NCB), New South Wales (NSW) is one of only a handful of coastal dunefields where short-term migration rates have been studied.

Two studies have been undertaken, by the Public Works Department (1977) and Robson *et al.* (1993), of which the work of Robson and Hunt used a more accurate methodology. They analysed the migration of dunes within the Newcastle Bight (NCB) over a 29 year period (1951-1983) using a mixture of aerial photographs and repeated topographic transects. They found an overall rate of sand drift for the NCB of 4.1 m/yr in a NNW direction, with rates varying between -0.7 to 8.4 m. Within the southern NCB this rate averaged 0.8 m/yr. Within the inland extension of the actively migrating current generation of dunes (the 'arm') they found a more easterly sand drift direction (except the most coastward part of the arm which experienced a northerly migration).

The modelling of wind drift potential has been used to help explain dune morphological variability and migration rates (Fryberger, 1979; Levin *et al.*, 2014; Robson *et al.*, 1993). A study undertaken by Levin *et al.* (2014) explored the spatial variability of wind speed and direction around Moreton Island, Queensland and its relation to the evolution of slipfaces within its dunefields. They highlighted the importance of the location of weather stations when estimating sand movement to explore the variability seen in dune orientation, as both wind speed and direction is highly spatially variable along and inland from the coast. The goal of this study is to quantify the rates, geomorphic processes and direction of the short term migration seen within the current generation of dunes within the southern NCB and its

relationship to observed winds. The results will be compared with previous migration estimates made by Robson *et al.* (1993).

Studies exploring the short-medium term evolution of coastal dunefields offer important insights that can help underpin strategic coastal management to ensure that the important biodiversity and cultural heritage values of these systems are preserved and that infrastructure built upon these systems is sustainable (Worimi Conservation Lands, 2015).

3.2 Regional Setting

The NCB is ~130 km north of Sydney and resides within the co-managed Worimi National Park and Worimi Conservation Lands. The dunefield has significant cultural heritage with numerous aboriginal artefacts being located during erosional events, sand mining and research activities. Thom *et al.* (1992) conducted an in-depth study of the geomorphology of the NCB, suggesting that the dunefield was formed in three stages during the Holocene, resulting in the formation of three dune generations (see Figure 1). A large part of the dunefield, the 'current generation', is bare and mobile and represents the largest active coastal dunefield within NSW (Robson *et al.*, 1993). The two older generations of dunes are currently well vegetated. A recent analysis of a LiDAR-derived DEM within the area (Paper One-Chapter Two) has highlighted that there is significant variability in both dune height and volume seen within the current generation dunes and an increase in sediment height and volume within the northern region as compared with the southern region. Dune slope azimuths were found to align at ~40 degrees oblique to the coastline orientation with an almost equal distribution between the ESE (52.6%) and WNW (47.4%) within the northern current generation suggesting dune migration both along the beach and inland. Within the southern current generation this relationship is altered so that there is a slight dominance of the ESE (55.6%) over the west (44.4%) with a shift slightly to the south in both components as compared with the north.

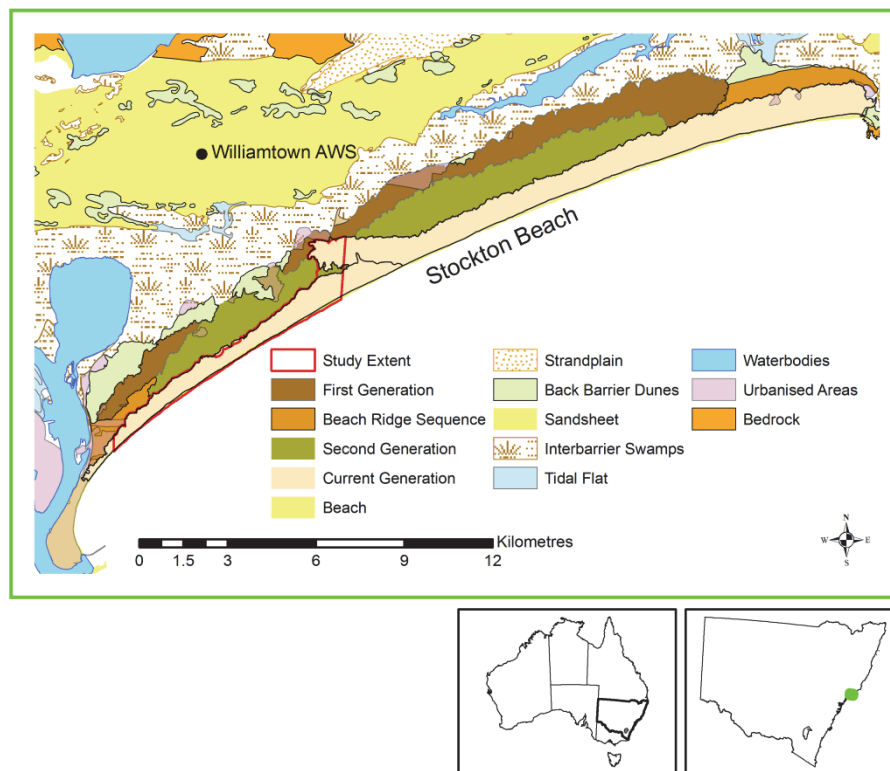


Figure 1: Geomorphic map of NCB. **Note:** the extent of overlapping LiDAR is shown in red. The geomorphic units/dune generations were modified from Thom et al. (1992). The map was modified by incorporating the analysis of aerial imagery and LiDAR derived DEMs.

The NCB has had a history of significant anthropogenic modification (see Fig. 1). Alterations include the establishment of a number of sand mines, the recent expansion of housing developments within the first and second dune generations and use of the southern end of the foredune as a military proving ground (Worimi Conservation Lands, 2015). Parts of the current generation within the southern NCB are used for recreational activities (4WD and ATV), the continuation of which relies upon the protection of this system (Worimi Conservation Lands, 2015). All areas of visible anthropogenic alteration have been removed from the analyses undertaken within this study. The focus of this study will be on the current generation dunes including the foredune complex. A sand mining operation established in 2015 on the northern region of the transverse arm at the northern extent of this study is beyond the time period of the LiDAR surveys. The findings of this study may be of importance to a housing development within the second generation which has expanded towards the actively migrating foredune complex.

3.3 Methods

This study utilises a novel crest mapping approach outlined in the companion paper (Chapter 2). This approach uses a GRASSGIS (GRASS Development Team, 2015) script developed by Jasiewicz and Stepinski (2013), which utilises Local Ternary Patterns (LTP) to adaptively map topographic features

using a DEM integrated with an ArcGIS basin analysis. This method offers an approach relatively free from user-subjectivity.

The LiDAR-derived DEMs utilised within this study were collected by the NSW Government department of Land and Primary Industry (LPI) to explore the effects of rising sea levels upon the coast (NSW Department of Planning, 2008). These DEMs offer a high resolution (1x1 – 2x2 m cells) and high accuracy bare-earth model of NCB and include two overlapping regions within the southern end of the embayment. The DEMs that are utilised in this study and their acquisition dates are shown in Table 1. Due to variability in cell size between the DEMs the Port Stephens and Raymond Terrace DEMs were resampled with a bilinear resample within ArcGIS to meet the lower resolution Hunter DEM. This method has been suggested as the optimal model for DEM resampling by Tao *et al.* (2008).

Table 1: LiDAR derived DEM datasets utilised in this study. **Note:** The Raymond Terrace and Port Stephens DEMs were resampled using Bilinear resample (see Appendix 1 for more information). The Port Stephens and Raymond Terrace DEMs were resampled to the resolution of the Hunter DEM so that volumetric and crestlines were comparable between the datasets. All DEMs were created using multiple flights to acquire the necessary density of returns and as such each DEM has a date range.

LiDAR DEM dataset	Acquisition Date	Cell size (m x m)
Port Stephens	15/12/2012- 16/06/2013	1 x 1
Raymond Terrace	16/06/2013- 07/07/2013	1 x 1
Hunter	1/01/2007-31/01/2007	2 x 2

Daily wind speed observations (9 am and 3 pm wind speed and direction) acquired from the Bureau of Meteorology automatic weather station at Williamtown Airport (located 6.5 km inland, 9 m.a.s.l.) were used to calculate total sand drift potential (DP), resultant sand drift potential (RDP) and resultant drift directions (RDD) following a modification of the (Fryberger, 1979) method after (Hesse *et al.*, 2017). Due to the restriction of two daily measurements the analyses undertaken within this report are likely an underestimate of total sand movement as the two daily measurements likely miss out on brief periods of strong winds that disproportionately contribute to DP. RDP and DP values were calculated as mean daily, monthly (30 days) and yearly (365 days) vectors during the study period and RDD were plotted using un-binned directional data.

Volumetric analyses will be undertaken through the Raster Calculator tool within ArcMap (ESRI, 2014). Any regions with volume changes within the derived DEM error margin will be resampled to zero change detected.

3.4 Results

3.4.1 LiDAR Accuracy

To estimate the inherent accuracy of the DEMs used within this study, sample points from the overlapping DEMs within the Port Stephens/Raymond Terrace and Hunter DEMs which should have experienced minimal change between the DEM acquisition's (in this case sealed roads) were digitised

and their elevations compared (Fig. 2 a, b). The mean difference between the DEMs is ~8.6 cm with a standard deviation of ~8.2 cm between the Port Stephens and Hunter DEMs (Fig. 2 a). In contrast, the mean difference between the Raymond Terrace and Hunter DEM is ~2.3 cm with a standard deviation of ~4.5 cm (Fig. 2 b). The apparent variability between derived accuracy is likely due to a smaller sample size being used within the Raymond Terrace overlap. These values are within the range expected from the provider (that stated a vertical error of 15 cm RMSE, NSW Department of Planning (2008)). Consequently this study utilised their more conservative RMSE vertical accuracy ~15 cm as the analyses undertaken within this study are considered to be the best case scenario and likely underestimate the error found within vegetated or more topographically variable surfaces.

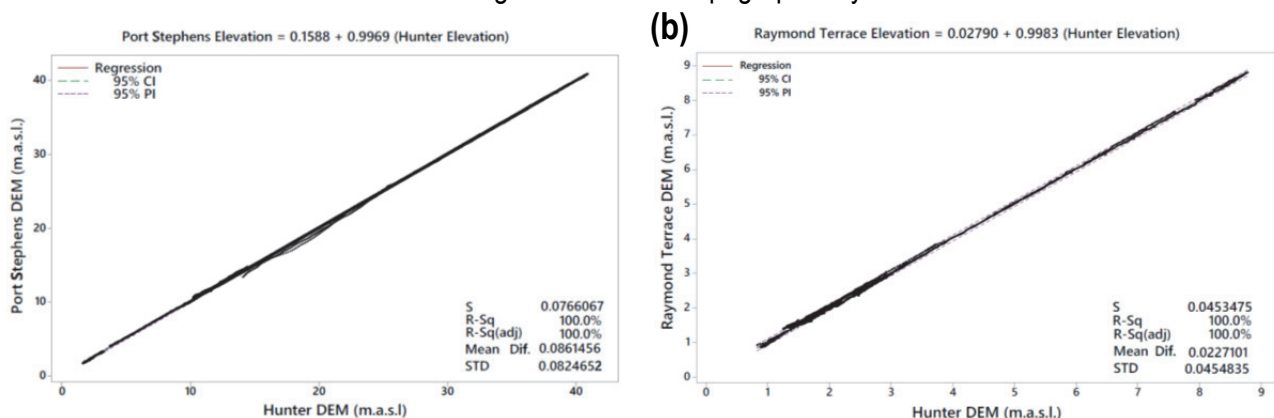


Figure 2: Regression analysis of vertical accuracy of LiDAR derived datasets within the NCB dunefield. (a) Port Stephens and Hunter DEMs (b) Raymond Terrace and Hunter DEMs. Points were extracted from locations that experienced minimal change between LiDAR acquisition dates (i.e. sealed roads). Vertical accuracy noted concerns the final filtered dataset not the DEM provided by the LPI. Mean Diff. = Mean Difference STD= Standard deviation of mean difference.

3.4.2 Crest mapping

The accuracy of automatically derived crests was assessed through the visual comparison of automated crestlines with a series of topographic transects undertaken throughout the dunefield. Visual analysis of the final product found that dunes with erosional surfaces (hollows) and poorly-defined crests were less clearly identified because they were modelled as valley slopes not crestlines. Due to the reliance upon ArcMap basin tool, all crestlines derived within this approach must represent locations that have no cells flowing into them and thus the detections of false positives should be minimal.

Figure 3 shows the migration of dune crests larger than 1 m (above the nearest interdune) between the various LiDAR acquisitions. There is an increase in both crest number and crest definition towards the northeast. There is also a obvious and consistent pattern of eastward migration of dune crests in 2013 when compared with 2007 (Fig. 3). However, crest migration on the arm and low elevation foredunes is significantly lower than the taller hind dunes.

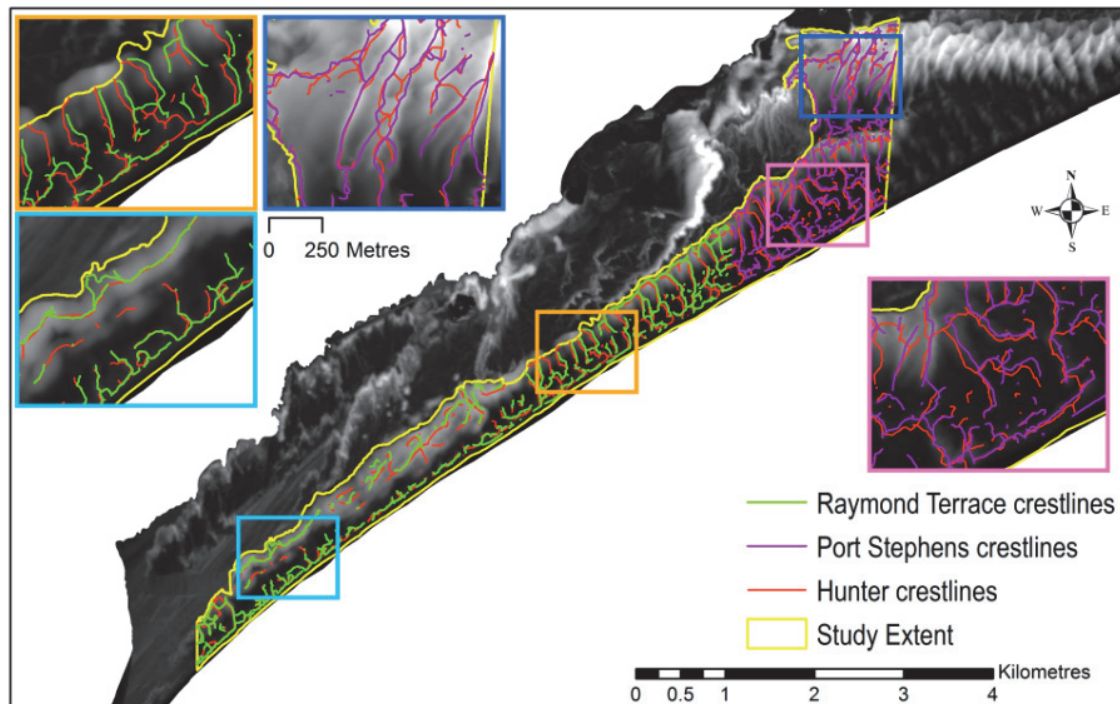


Figure 3: Crest migration within the current generation of the southern NCB derived from automated crest mapping.

3.4.3 Volumetric analysis of sand movement

The normalised volumetric change along the southern NCB (Fig. 4) shows two major directions of sand movement: (1) a dominant northerly movement of sand at the landward margin of the dune body and, (2) a north-eastern movement of sand along the beach. There is no detectable sand movement within the depression between the arm and the main southern dune body. This depression is dominated by swamp and vegetation and is largely stabilised.

3.4.4 Resultant Drift Direction (RDD)

RDD wind roses (Fig. 5 a, b) predict a northward and north-westward movement of sand from onshore winds during the total study period and during summer (within the study period) respectively. In winter (Fig 5 c), offshore winds dominate and result in a narrow mode of RDD from the WNW. Summer, autumn and spring were found to be responsible for the majority of onshore and northerly alongshore movement of sand within the NCB.

During the study period there were two main RDDs at Williamtown (Fig. 6a); a relatively stable west-northwest RDD during the period from May-August and a more variable ESE to southerly RDD during October-April. The mean monthly DP shown in Figure 6 (b) shows a peak in DP during the period July-October with a decreasing trend between November and June, suggesting that the main sand moving months occur during late winter and all of spring when the RDD swings from WNW through S to SE.

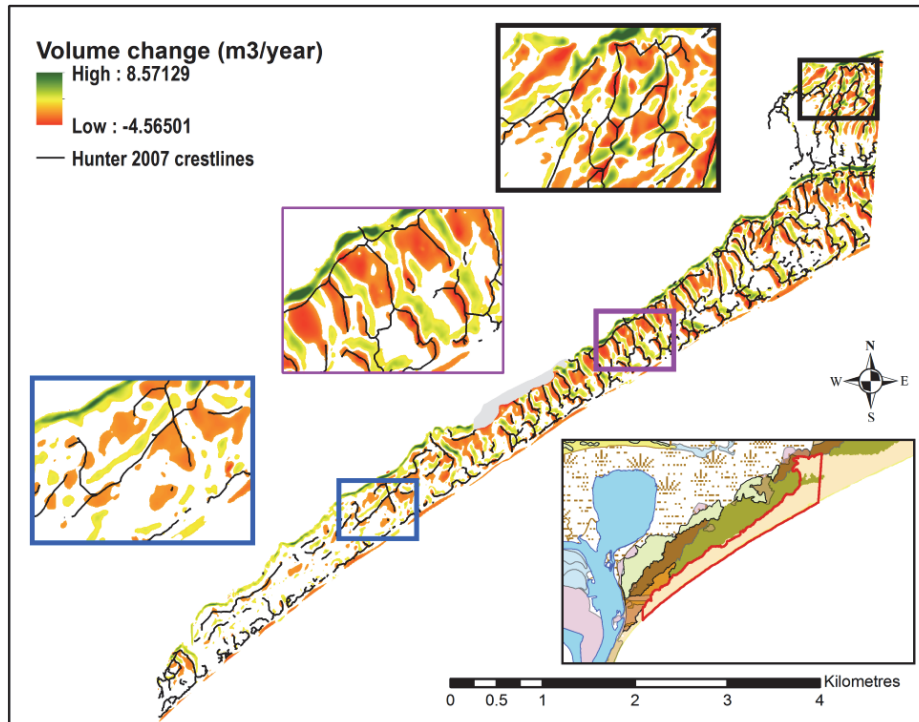


Figure 4: Normalised annual volumetric change along southern Stockton Beach (NCB) current generation. **Note:** the region denoted in grey has been removed from this analysis due to bulk removal of sediment to build an access road and regions denoted in white are areas with no change (i.e. cells with values within the DEM error margin). As error has not been removed from all cell values the volume change shown in this figure should be considered as relative change.

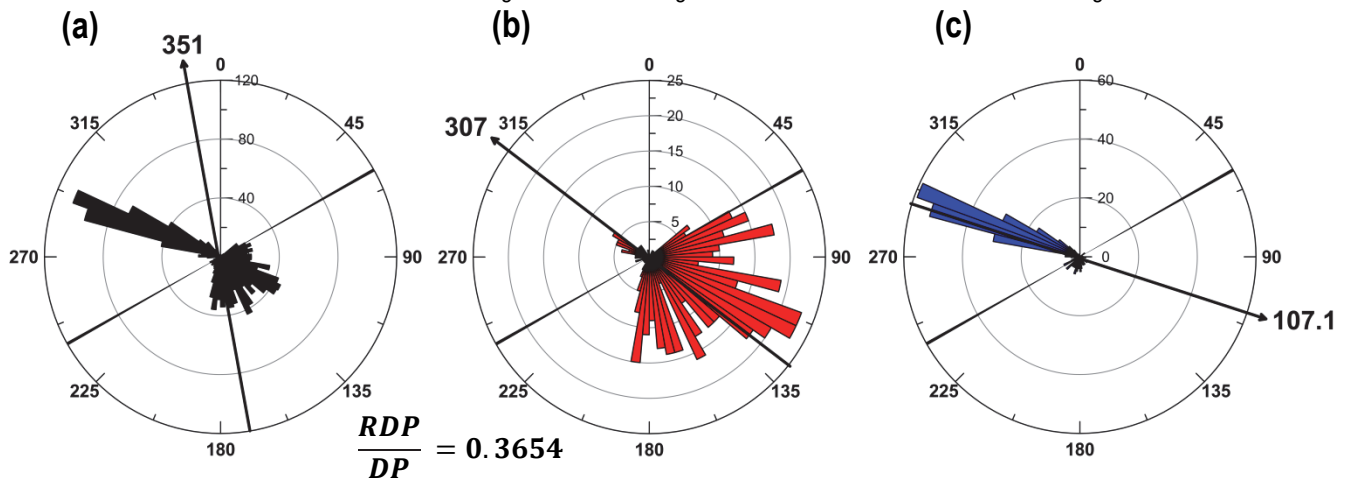


Figure 5: RDD graphs for (a) Annual, (b) Summer, and (c) Winter during the study period January 2007-July 2013 (created using daily RDD data). The arrows represent the median RDD for each period and RDP/DP is shown underneath the figures. **Note:** The rose plots have different frequency scales to improve legibility. Spring and Autumn had plots showing a transition from the Summer and Winter and can be found in Appendix 6. Created from wind data collected by the Bureau of Meteorology from Williamtown AWS.

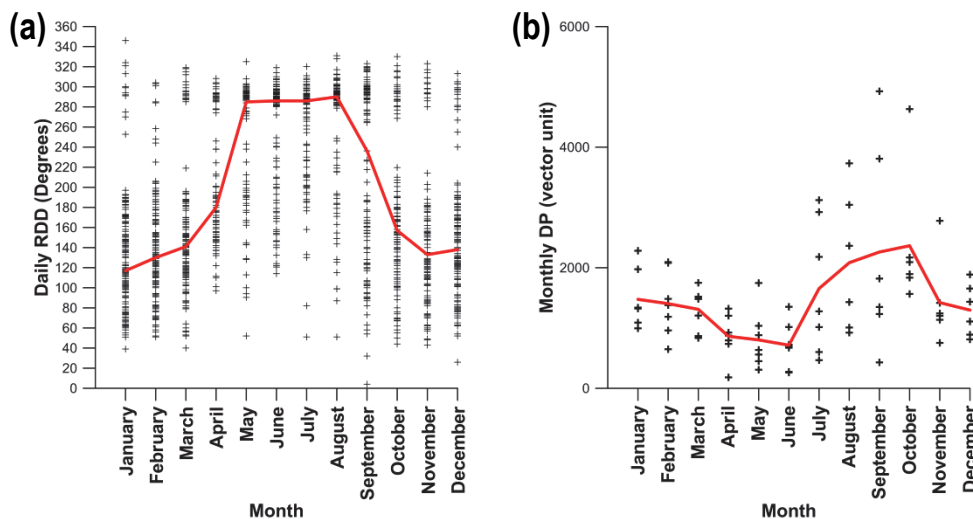


Figure 6: (a) Daily RDD with median monthly RDD shown in red, and (b) Monthly DP with mean DP shown in red for the study period January 2007-July 2013 calculated from wind data collected by the Bureau of Meteorology Williamtown AWS.

3.5 Discussion

Visual analysis of satellite imagery acquired during the study period shows a strong relationship between the areas of no crest change and low-lying areas of swamps. This is possibly a modern analogue to the process suggested by Thom *et al.* (1992) whereby regions close to the water table, such as those found within the low elevation sand sheet within the Seal Rocks dunefield, act as a surface across which there is significant movement of sand forming downwind dune features.

The volume change relationships and the DP and RDD extracted from the nearby Williamtown AWS provide consistent directions in sand movement with (1) a dominant northwesterly movement of sand to the landward side of the barrier, in foredunes and in dunes of the 'arm', and, (2) a north-easterly movement of transverse hind dunes (Fig. 5 a,b,c). However, the morphology of the dunes suggest that similar to the findings of Levin *et al.* (2014) onshore winds likely play a larger role for coastal dune formation than offshore winds. In the case of the NCB this relationship is especially true as the DP of offshore easterly winds is likely to be diminished due to the significant interaction and roughness caused by the older and now vegetated first and second generation barriers. If the winds do make it through to the current generation the DP is likely to be minimal due to the significant incline of the current generation barrier slipface.

Sand movement within the northern end of the study area is greater than that experienced in the south, in agreement with the findings of Robson *et al.* (1993). In all areas of the barrier both the NW movement of SW-NE aligned crests and the NE movement of NW-SE aligned dunes can be seen, although the relative dominance of these two dune sets and transport directions changes along the barrier. Robson *et al.* (1993) suggested a northward movement and presence of reversing transverse dunes in this location. Our findings suggest a more complex movement of two intersecting sets of

dunes, rather than reversing dunes. Dune crest migration is most visible alongshore and to the northeast (Fig. 3), whilst crest migration directly inland (NW) is less noticeable. The greater height of these dunes means that large volumes of sand movement are accommodated with relatively small/slow dune crest movement. Consequently, it is likely that due to the large volumes stored within the longwall transgressive dune running along the landward extent of the current barrier that it would take extended periods of time for the crest to migrate inland.

Assuming that gross wind direction patterns have not changed since the Holocene, summer and winter appear to be the main seasons that have the largest direct impact on the alteration of the 'arm' with summer (24.03% total study DP) having the greatest effect on arm extension through onshore movement of sand and, winter (34.38% total study DP) through obliquely offshore movement (to the east) of sand. This may result in a seasonal/periodic dune reversal on the arm likely dampening its migration inland, to the west. This finding is supported by those of Robson *et al.* (1993) who found sampled dunes to reverse periodically and to be largely immobile due to the presence of a moist sand core. However, due to the dominance (~10% greater DP) of the winter seasons upon the arm this would result in a trend of slip faces towards the coast (which is not evident within the dune orientations).

3.6 Conclusions

Analysis of overlapping LiDAR derived DEMs within the NCB has shown a coherent pattern of dune crest movement and volume change over the period from 2007 to 2013. Two sets of intersecting dunes were found: SW – NE oriented dunes which moved towards the NW and NW-SE oriented dunes which moved towards the NE. These movements are explained by the pattern of RDD and DP derived from the nearby Bureau of Meteorology weather station (Williamstown AWS) and are largely consistent with the findings of (Robson *et al.*, 1993). It is likely that the inland location of the Williamstown AWS underestimates the wind drift potential of the onshore and alongshore winds due to it being located 6.5 km inland and behind the dunefield barriers. The style of dune movement (two intersecting sets of transverse dunes), driven by seasonally alternating winds, is a complex dunefield organisation distinct from nearby parabolic dunes or reversing dunes found elsewhere and previously ascribed to this site Robson *et al.* (1993).

This study has also highlighted the value of LiDAR derived analyses of dune migration and it is highly recommended that the periodic acquisition of LiDAR dataset be undertaken to aid our understanding and management of these systems into the future.

3.7 Acknowledgements

This research was funded by a Macquarie University postgraduate research fund (Farebrother). We would like to thank the Bureau of Meteorology for providing the AWS data from Williamtown AWS and the LPI for providing the LiDAR-derived DEMs.

Chapter 4: Thesis conclusions and recommendations for further study

This research has highlighted that coastal dunefields are complex features and their morphologies show the complex integration of sand supply, vegetation dynamics and variations in climate and sea level. This thesis has introduced a novel crest mapping approach which can be used in a diverse range of dunefields where bare-surface DEMs are available and can offer crucial insights into the morphology and subsequent evolution of these systems.

The lack of major orientation changes within the various parabolic dune and transverse dune generations within all the study sites suggests either wind direction has not changed substantially or that the broad scatter of dune orientations prevents detection of relatively minor changes in wind direction. It is possible that variations in swell and wave direction contributed to the changes in sediment supply to these dunefield but are not detectable within the dunes themselves.

The dunefields explored within this study show different sediment supply regimes during the late Holocene with SR supporting the decrease in sediment supply suggested by earlier studies (Davies, 1986, Short, 1988, Short and Hesp, 1982). In contrast, the Booderee dunefield shows the likelihood that sand supply increased over the late Holocene and the NCB strongly suggests an increase in supply supporting the findings of Oliver *et al.* (2015) and Goodwin *et al.* (2006) elsewhere on the NSW coast.

Through the analysis of multi-temporal LiDAR the short-term migration of dunes within the southern NCB current generation was explored between 2007-2013. Two sets of intersecting dunes were found: SW – NE oriented dunes which moved towards the NW and NW-SE oriented dunes which moved towards the NE. These insights into short-term dune migration may help to inform future management strategies within this system.

This research has highlighted that strategic dating is needed to help to constrain the temporality of the evolution of these systems. Likewise a large series of repeated LiDAR acquisitions are needed to help us understand how these systems operate in the short-term. This will enable us to better understand our effects on these systems (both directly and indirectly) and how to help protect them from climate change.

Future studies concerning coastal compartment size and previous wave directionality is expected to be of great importance to aid in the understanding of sand supply interactions over long-term (i.e. since dunefield formation during the Holocene) and as such are suggested as key areas for future research.

Chapter 5: References

- AAGAARD, T., DAVIDSON-ARNOTT, R., GREENWOOD, B. & NIELSEN, J. (2004), Sediment supply from shoreface to dunes: linking sediment transport measurements and long-term morphological evolution, *Geomorphology*, 60 (1–2), 205–224, <http://dx.doi.org/10.1016/j.geomorph.2003.08.002>
- AL-MASRAHY, M. A. & MOUNTNEY, N. P. (2013), Remote sensing of spatial variability in aeolian dune and interdune morphology in the Rub' Al-Khali, Saudi Arabia, *Aeolian Research*, 11 155–170, <http://dx.doi.org/10.1016/j.aeolia.2013.06.004>
- ANDREWS, B. D., GARES, P. A. & COLBY, J. D. (2002), Techniques for GIS modeling of coastal dunes, *Geomorphology*, 48 (1–3), 289–308, [http://dx.doi.org/10.1016/S0169-555X\(02\)00186-1](http://dx.doi.org/10.1016/S0169-555X(02)00186-1)
- BAAS, A. C. W. (2002), Chaos, fractals and self-organization in coastal geomorphology: simulating dune landscapes in vegetated environments, *Geomorphology*, 48 (1–3), 309–328, [http://dx.doi.org/10.1016/S0169-555X\(02\)00187-3](http://dx.doi.org/10.1016/S0169-555X(02)00187-3)
- BAAS, A. C. W. & NIELD, J. M. (2007), Modelling vegetated dune landscapes, *Geophysical Research Letters*, 34 (6), n/a-n/a, 10.1029/2006GL029152
- BAAS, A. C. W. & NIELD, J. M. (2010), Ecogeomorphic state variables and phase-space construction for quantifying the evolution of vegetated aeolian landscapes, *Earth Surface Processes and Landforms*, 35 (6), 717–731, 10.1002/esp.1990
- BAILEY, S. D. & BRISTOW, C. S. (2004), Migration of parabolic dunes at Aberffraw, Anglesey, north Wales, *Geomorphology*, 59 (1–4), 165–174, <http://dx.doi.org/10.1016/j.geomorph.2003.09.013>
- BAITIS, E., KOCUREK, G., SMITH, V., MOHRIG, D., EWING, R. C. & PEYRET, A. P. B. (2014), Definition and origin of the dune-field pattern at White Sands, New Mexico, *Aeolian Research*, 15 269–287, <http://dx.doi.org/10.1016/j.aeolia.2014.06.004>
- BARCHYN, T. E. & HUGENHOLTZ, C. H. (2012a), Predicting vegetation-stabilized dune field morphology, *Geophysical Research Letters*, 39 (17), n/a-n/a, 10.1029/2012GL052905
- BARCHYN, T. E. & HUGENHOLTZ, C. H. (2012b), A process-based hypothesis for the barchan–parabolic transformation and implications for dune activity modelling, *Earth Surface Processes and Landforms*, 37 (13), 1456–1462, 10.1002/esp.3307
- BARROS, A. M. G., PEREIRA, J. M. C. & LUND, U. J. (2012), Identifying geographical patterns of wildfire orientation: A watershed-based analysis, *Forest Ecology and Management*, 264 98–107, <http://dx.doi.org/10.1016/j.foreco.2011.09.027>
- BAUER, B. O. & DAVIDSON-ARNOTT, R. G. D. (2003), A general framework for modeling sediment supply to coastal dunes including wind angle, beach geometry, and fetch effects, *Geomorphology*, 49 (1–2), 89–108, [http://dx.doi.org/10.1016/S0169-555X\(02\)00165-4](http://dx.doi.org/10.1016/S0169-555X(02)00165-4)
- BAUER, B. O., DAVIDSON-ARNOTT, R. G. D., HESP, P. A., NAMIKAS, S. L., OLLERHEAD, J. & WALKER, I. J. (2009), Aeolian sediment transport on a beach: Surface moisture, wind fetch, and mean transport, *Geomorphology*, 105 (1–2), 106–116, <http://dx.doi.org/10.1016/j.geomorph.2008.02.016>
- BISHOP, M. A. (2010), Nearest neighbor analysis of mega-barchanoid dunes, Ar Rub' al Khali, sand sea: The application of geographical indices to the understanding of dune field self-organization, maturity and environmental change, *Geomorphology*, 120 (3–4), 186–194, <http://dx.doi.org/10.1016/j.geomorph.2010.03.029>
- BLUMBERG, D. G. (2006), Analysis of large aeolian (wind-blown) bedforms using the Shuttle Radar Topography Mission (SRTM) digital elevation data, *Remote Sensing of Environment*, 100 (2), 179–189, <http://dx.doi.org/10.1016/j.rse.2005.10.011>
- BOLEYN, D. A. & CAMPBELL, B. L. 1966. Littoral Drift in the Vicinity of Newcastle Harbour Entrance. Department of Public Works NSW Australia, Harbours and Rivers Branch, Manly Hydraulic and Soils Laboratory and Australian Atomic Energy Commission.

- BOWMAN, G. M. (1989), Podzol Development in a Holocene Chronosequence. I. Moruya Heads, New South Wales, *Australian Journal of Soil Research*, 27 607-628,
- BRISTOW, C. S., DULLER, G. A. T. & LANCASTER, N. (2007), Age and dynamics of linear dunes in the Namib Desert, *Geology*, 35 (6), 555-558, 10.1130/g23369a.1
- BULLARD, J. E., THOMAS, D. S. G., LIVINGSTONE, I. & WIGGS, G. F. S. (1995), Analysis of linear sand dune morphological variability, southwestern Kalahari desert, *Geomorphology*, 11 (3), 189-203, [http://dx.doi.org/10.1016/0169-555X\(94\)00061-U](http://dx.doi.org/10.1016/0169-555X(94)00061-U)
- BUREAU OF METEOROLOGY 2016. Climate Statistics for Australian Locations. In: BUREAU OF METEOROLOGY (ed.).
- CARTA, J. A., BUENO, C. & RAMÍREZ, P. (2008), Statistical modelling of directional wind speeds using mixtures of von Mises distributions: Case study, *Energy Conversion and Management*, 49 (5), 897-907, <http://dx.doi.org/10.1016/j.enconman.2007.10.017>
- CARTER, R. W. G. (1991), Near-future sea level impacts on coastal dune landscapes, *Landscape Ecology*, 6 (1/2), 29-39,
- CAZENAVE, P. W., DIX, J. K., LAMBKIN, D. O. & MCNEILL, L. C. (2013), A method for semi-automated objective quantification of linear bedforms from multi-scale digital elevation models, *Earth Surface Processes and Landforms*, 38 (3), 221-236, 10.1002/esp.3269
- DAVIES, J. L. 1986. The Coast. In: JEANS, D. N. (ed.) *Australia: A Geographic, v 1, The Natural Environment*. Sydney: Sydney University Press.
- DEL ANGEL, D. 2012. *Dune-beach morphodynamic interaction along a semi-arid, wave dominated barrier island: South Padre Island, Texas*. Masters Degree of Science Masters, Texas A&M University-Corpus Christi.
- DERICKSON, D., KOCUREK, G., EWING, R. C. & BRISTOW, C. (2008), Origin of a complex and spatially diverse dune-field pattern, Algodones, southeastern California, *Geomorphology*, 99 (1-4), 186-204, <http://dx.doi.org/10.1016/j.geomorph.2007.10.016>
- DOYLE, T. B. & WOODROFFE, C. D. Investigating foredune morphodynamics and ecology using Airborne LiDAR in SE Australia. 24th Coastal Conference 2015, 2015. 13.
- DULLER, G. A. T. 2008. *Luminescence Dating: guidelines on using Luminescence dating in archaeology*, Swindon, English Heritage.
- DURÁN, O. & MOORE, L. J. (2013), Vegetation controls on the maximum size of coastal dunes, *Proceedings of the National Academy of Sciences*, 110 (43), 17217-17222, 10.1073/pnas.1307580110
- ENVI 2015. ENVI 5.2.1 ed. Boulder, Colorado: Exelis Visual Information Solutions.
- ESRI 2014. ArcGIS Desktop: Release 10.3. . Redlands, CA: Environmental Systems Research Institute.
- EWING, R. C. & KOCUREK, G. (2010), Aeolian dune-field pattern boundary conditions, *Geomorphology*, 114 (3), 175-187, <http://dx.doi.org/10.1016/j.geomorph.2009.06.015>
- EWING, R. C., KOCUREK, G. & LAKE, L. W. (2006), Pattern analysis of dune-field parameters, *Earth Surface Processes and Landforms*, 31 (9), 1176-1191, 10.1002/esp.1312
- FERREIRA, M. 2014. *Perpendicular Transects (Ferreira)* [Online]. Available: <http://gis4geomorphology.com/stream-transects-partial/> [Accessed Dec 2014].
- FRYBERGER, S. G. 1979. Dune forms and wind regime. In: MCKEE, E. D. (ed.) *A Study of Global Sand Seas*. Washington: USGS.
- GALLANT, J. (2011), Adaptive smoothing for noisy DEMs, *Geomorphometry.org*, 37-40,
- GOODWIN, I. D., STABLES, M. A. & OLLEY, J. M. (2006), Wave climate, sand budget and shoreline alignment evolution of the Iluka-Woody Bay sand barrier, northern New South Wales, Australia, since 3000 yr BP, *Marine Geology*, 226 (1-2), 127-144, <http://dx.doi.org/10.1016/j.margeo.2005.09.013>
- GRACIA, J., DEL RIO, L., ALONSO, C., BENAVENTE, J. & ANFUSO, G. (2006), Historical evolution and present state of the coastal dune systems in the Atlantic coast of Cadiz (SW Spain): palaeoclimatic and environmental implications. , *Coastal Geomorphology in Spain. Proc. of the III Spanish Conference on Coastal Geomorphology: J. Coastal Research S.I.*, 48 55-63,

- GRASS DEVELOPMENT TEAM 2015. Geographic Resources Analysis Support System (GRASS) Software. 7 ed.: Open Source Geospatial Foundation.
- GRIFFIN, J. D., HEMER, M. A. & JONES, B. G. (2008), Mobility of sediment grain size distributions on a wave dominated continental shelf, southeastern Australia, *Marine Geology*, 252 (1–2), 13–23, <http://dx.doi.org/10.1016/j.margeo.2008.03.005>
- HACK, J. T. (1941), Dunes of the Western Navajo Country, *Geographical Review*, 31 (2), 240–263, 10.2307/210206
- HANSON, P. R., MASON, J. A., JACOBS, P. M. & YOUNG, A. R. (2015), Evidence for bioturbation of luminescence signals in eolian sand on upland ridgetops, southeastern Minnesota, USA, *Quaternary International*, 362 108–115, <http://dx.doi.org/10.1016/j.quaint.2014.06.039>
- HESP, P. A. (1991), 5: Ecological processes and plant adaptations on coastal dunes, *Journal of Arid Environments*, 21 165–191,
- HESP, P. A. (2002), Foredunes and blowouts: initiation, geomorphology and dynamics, *Geomorphology*, 48 (1–3), 245–268, [http://dx.doi.org/10.1016/S0169-555X\(02\)00184-8](http://dx.doi.org/10.1016/S0169-555X(02)00184-8)
- HESP, P. A. (2004), 3 Coastal Dunes in the Tropics and Temperate Regions: Location, Formation, Morphology and Vegetation Processes, *Ecological Studies*, 171 29–49,
- HESP, P. A. Surfzone-beach-dune interactions. In: KRANENBURG, W. M., HORSTMAN, E. M. & WIJNBERG, K. M., eds. NCK – days 2012: Crossing Borders in Coastal Research: Jubilee Conference Proceedings, 2012 Enschede, the Netherlands. 35–40.
- HESP, P. A. (2013), Conceptual models of the evolution of transgressive dune field systems, *Geomorphology*, 199 138–149, <http://dx.doi.org/10.1016/j.geomorph.2013.05.014>
- HESP, P. A. & THOM, B. G. 1990. Geomorphology and evolution of active transgressive dunefields. In: NORDSTROM, K. F., PSUTY, N. P. & CARTER, R. W. G. (eds.) *Coastal dunes: form and process*. London: Wiley.
- HESSE, P., MATT, T. & FAREBROTHER, W. (2017), Complexity confers stability: Climate variability, vegetation response and sand transport on longitudinal sand dunes in Australia's deserts, *Aeolian Research*, 25 45–61, <http://dx.doi.org/10.1016/j.aeolia.2017.02.003>
- HORNIK, K. & GRUEN, B. (2014), movMF: An R Package for Fitting Mixtures of von Mises-Fisher Distributions, *Journal of Statistical Software*, 58 (10), 1–31,
- HOUSER, C. & MATHEW, S. (2011), Alongshore variation in foredune height in response to transport potential and sediment supply: South Padre Island, Texas, *Geomorphology*, 125 (1), 62–72, <http://dx.doi.org/10.1016/j.geomorph.2010.07.028>
- HUGENHOLTZ, C. H., LEVIN, N., BARCHYN, T. E. & BADDOCK, M. C. (2012), Remote sensing and spatial analysis of aeolian sand dunes: A review and outlook, *Earth-Science Reviews*, 111 (3–4), 319–334, <http://dx.doi.org/10.1016/j.earscirev.2011.11.006>
- JASIEWICZ, J. & STEPINSKI, T. F. (2013), Geomorphons — a pattern recognition approach to classification and mapping of landforms, *Geomorphology*, 182 147–156, <http://dx.doi.org/10.1016/j.geomorph.2012.11.005>
- JENNINGS, J. N. (1957), On the Orientation of Parabolic or U-Dunes, *The Geographical Journal*, 123 (4), 474–480, 10.2307/1790349
- KEIJERS, J. G. S., DE GROOT, A. V. & RIKSEN, M. J. P. M. (2015), Vegetation and sedimentation on coastal foredunes, *Geomorphology*, 228 723–734, <http://dx.doi.org/10.1016/j.geomorph.2014.10.027>
- KIDD, R. 2001. *Coastal Dune Management: A Manual of Coastal Dune Management and Rehabilitation Techniques*, DLWC, Newcastle, NSW Department of Land and Water Conservation.
- KOCUREK, G. & EWING, R. C. (2005), Aeolian dune field self-organization – implications for the formation of simple versus complex dune-field patterns, *Geomorphology*, 72 (1–4), 94–105, <http://dx.doi.org/10.1016/j.geomorph.2005.05.005>
- LEES, B. (2006), Timing and Formation of Coastal Dunes in Northern and Eastern Australia, *Journal of Coastal Research*, 22 (1), 78–89,

- LEVIN, N., NEIL, D. & SYKTUS, J. (2014), Spatial variability of dune form on Moreton Island, Australia, and its correspondence with wind regime derived from observing stations and reanalyses, *Aeolian Research*, 15 289-300, <http://dx.doi.org/10.1016/j.aeolia.2014.06.006>
- LEWIS, S. E., SLOSS, C. R., MURRAY-WALLACE, C. V., WOODROFFE, C. D. & SMITHERS, S. G. (2013), Post-glacial sea-level changes around the Australian margin: a review, *Quaternary Science Reviews*, 74 115-138, <http://dx.doi.org/10.1016/j.quascirev.2012.09.006>
- LINDENMAYER, D., MACGREGOR, C., DEXTER, N., FORTESCUE, M. & BEATON, E. 2014. *Booderee National Park: The Jewel of Jervis Bay*, Collingwood Victoria, CSIRO Publishing.
- LITHGOW, D., MARTÍNEZ, M. L., GALLEGU-FERNÁNDEZ, J. B., HESP, P. A., FLORES, P., GACHUZ, S., RODRÍGUEZ-REVELO, N., JIMÉNEZ-OROCIO, O., MENDOZA-GONZÁLEZ, G. & ÁLVAREZ-MOLINA, L. L. (2013), Linking restoration ecology with coastal dune restoration, *Geomorphology*, 199 214-224, <http://dx.doi.org/10.1016/j.geomorph.2013.05.007>
- LUNA, M. C. M. D. M., PARTELI, E. J. R., DURÁN, O. & HERRMANN, H. J. (2009), Modeling transverse dunes with vegetation, *Physica A: Statistical Mechanics and its Applications*, 388 (19), 4205-4217, <http://dx.doi.org/10.1016/j.physa.2009.06.006>
- LUNA, M. C. M. D. M., PARTELI, E. J. R., DURÁN, O. & HERRMANN, H. J. (2011), Model for the genesis of coastal dune fields with vegetation, *Geomorphology*, 129 (3-4), 215-224, <http://dx.doi.org/10.1016/j.geomorph.2011.01.024>
- MASSERAN, N., RAZALI, A. M. & IBRAHIM, K. (2015), Application of mixtures of von Mises-Fisher model to investigate the statistical characteristics of the wind direction data, *WSEAS Transactions on Mathematics*, 14 313-323,
- MASSERAN, N., RAZALI, A. M., IBRAHIM, K. & LATIF, M. T. (2013), Fitting a mixture of von Mises distributions in order to model data on wind direction in Peninsular Malaysia, *Energy Conversion and Management*, 72 94-102, <http://dx.doi.org/10.1016/j.enconman.2012.11.025>
- MCKEE, E. D. 1979. A study of global sand seas. *Professional Paper*. U. S. Geological Survey
- MITASOVA, H., DRAKE, T. G., BERNSTEIN, D. & HARMON, R. S. (2004), Quantifying Rapid Changes in Coastal Topography using Modern Mapping Techniques and Geographic Information System, *Environmental & Engineering Geoscience*, 10 (1), 1-11, 10.2113/10.1.1
- MITASOVA, H., OVERTON, M. & HARMON, R. S. (2005), Geospatial analysis of a coastal sand dune field evolution: Jockey's Ridge, North Carolina, *Geomorphology*, 72 (1-4), 204-221, <http://dx.doi.org/10.1016/j.geomorph.2005.06.001>
- MONTAGUE, C. L. (2008), Recovering the Sand Deficity from a Century of Dredging and Jetties along Florida's Atlantic Coast: A Reevaluation of Beach Nourishment as an Essential Tool for Ecological Conservation, *Journal of Coastal Research*, 24 (4), 899-916, 10.2112/06-0710.1
- MUNYIKWA, K., BROWN, S. & KITABWALLA, Z. (2012), Delineating stratigraphic breaks at the bases of postglacial eolian dunes in central Alberta, Canada using a portable OSL reader, *Earth Surface Processes and Landforms*, 37 1603-1614, 10.1002/esp.3261
- NIELD, J. M. & BAAS, A. C. W. (2008), The influence of different environmental and climatic conditions on vegetated aeolian dune landscape development and response, *Global and Planetary Change*, 64 (1-2), 76-92, <http://dx.doi.org/10.1016/j.gloplacha.2008.10.002>
- NISHIMORI, H. & TANAKA, H. (2001), A simple model for the formation of vegetated dunes, *Earth Surface Processes and Landforms*, 26 (10), 1143-1150, 10.1002/esp.258
- NSW DEPARTMENT OF PLANNING 2008. High resolution terrain mapping of the NSW Central and Hunter coasts for assessments of potential climate change impacts: Final project report. NSW Department of Planning.
- OLIVER, T. S. N., DOUGHERTY, A. J., GLIGANIC, L. A. & WOODROFFE, C. D. (2015), Towards more robust chronologies of coastal progradation: Optically stimulated luminescence ages for the coastal plain at Moruya. souther-eastern Australia, *The Holocene*, 25 (3), 536-546,
- OTVOS, E. G. (2000), Beach ridges — definitions and significance, *Geomorphology*, 32 (1-2), 83-108, [http://dx.doi.org/10.1016/S0169-555X\(99\)00075-6](http://dx.doi.org/10.1016/S0169-555X(99)00075-6)

- OZCOASTS 2015. OzCoasts Australian Online Coastal Information: Database Simple Search. Geoscience Australia.
- PORTENGA, E. W. & BISHOP, P. (2016), Confirming geomorphological interpretations based on portable OSL reader data, *Earth Surface Processes and Landforms*, 41 (3), 427-432, 10.1002/esp.3834
- PUBLIC WORKS DEPARTMENT 1977. Sediment movement in the Newcastle Bight. In: GORDON, A. D. (ed.). Manly Hydraulics Laboratory
- PYE, K., SAYE, S. & BLOTT, S. 2007. Sand dune processes and management for flood and coastal defence- Part 2: Sand dune processes and morphology. *R&D Technical Report* London: Royal Holloway University of London, and Kenneth Pye Associates Ltd.
- R DEVELOPMENT CORE TEAM 2008. A language and environment for statistical computing. R Foundation for Statistical Computing, Vienna, Austria.
- ROBSON, R. O., COX, J. R., KILLERBY, M. C. & BAILEY, J. G. 1993. Newcastle Bight sand drift study (1985). In: HUNT, J. S. (ed.). Sydney: New South Wales. Department of Conservation and Land Management.
- ROY, P. S. (1999), Heavy mineral beach placers in southeastern Australia; their nature and genesis, *Economic Geology*, 94 (4), 567-588, 10.2113/gsecongeo.94.4.567
- RUST, I. C. & ILLENBERGER, W. K. (1996), Coastal dunes: sensitive or not?, *Landscape and Urban Planning*, 34 (3-4), 165-169, [http://dx.doi.org/10.1016/0169-2046\(95\)00232-4](http://dx.doi.org/10.1016/0169-2046(95)00232-4)
- SHARPLES, C., MOUNT, R., PEDERSEN, T., LACEY, M., NEWTON, J., JASKIERIAK, D. & WALLACE, L. 2009. The Australian coastal smartline geomorphic and stability map version 1. In: AUSTRALIA, A. D. O. C. C. A. G. (ed.) 1 ed. data.gov.au: data.gov.au.
- SHORT, A. D. (1988), Holocene coastal dune formation in southern Australia: A case study, *Sedimentary Geology*, 55 (1), 121-142, [http://dx.doi.org/10.1016/0037-0738\(88\)90093-0](http://dx.doi.org/10.1016/0037-0738(88)90093-0)
- SHORT, A. D. (2010a), Role of geological inheritance in Australian beach morphodynamics, *Coastal Engineering*, 57 (2), 92-97, <http://dx.doi.org/10.1016/j.coastaleng.2009.09.005>
- SHORT, A. D. (2010b), Sediment Transport around Australia-Sources, Mechanisms, Rates, and Barrier Forms, *Journal of Coastal Research*, 26 (3), 395-402,
- SHORT, A. D. & HESP, P. A. (1982), Wave, beach and dune interactions in southeastern Australia, *Marine Geology*, 48 (3), 259-284, [http://dx.doi.org/10.1016/0025-3227\(82\)90100-1](http://dx.doi.org/10.1016/0025-3227(82)90100-1)
- SLOSS, C. R., MURRAY-WALLACE, C. V. & JONES, B. G. (2007), Holocene sea-level change on the southeast coast of Australia: a review, *Holocene*, 17 (7), 999-1014,
- STEPINSKI, T. F. & JASIEWICZ, J. Geomorphons- A New Approach to Classification of Landforms. In: HENGL, T., EVANS, I. S., WILSON, J. P. & GOULD, M., eds. Proceedings of Geomorphometry, 30 May 2011 2011 Redlands, CA. 109-112.
- STOCKDON, H. F., DORAN, K. S. & SALLENGER, A. H. (2009), Extraction of Lidar-Based Dune-Crest Elevations for Use in Examining the Vulnerability of Beaches to Inundation During Hurricanes, *Journal of Coastal Research*, 25 (6), 59-65,
- SWANSON, T., MOHRIG, D. & KOCUREK, G. (2016), Aeolian dune sediment flux variability over an annual cycle of wind, *Sedimentology*, 63 (6), 1753-1764, 10.1111/sed.12287
- TAMURA, T. (2012), Beach ridges and prograded beach deposits as palaeoenvironment records, *Earth-Science Reviews*, 114 (3-4), 279-297, <http://dx.doi.org/10.1016/j.earscirev.2012.06.004>
- TAO, Y., TANG, G., JIA, Y. & GAO, Y. Research on Optimal Analysis Window Size and Resampling Method According to DEM Analysis Scale. Education Technology and Training, 2008. and 2008 International Workshop on Geoscience and Remote Sensing. ETT and GRS 2008. International Workshop on, 21-22 Dec. 2008 2008. 369-372.
- TELFER, M. W., FYFE, R. M. & LEWIN, S. (2015), Automated mapping of linear dunefield morphometric parameters from remotely-sensed data, *Aeolian Research*, 19, Part B 215-224, <http://dx.doi.org/10.1016/j.aeolia.2015.03.001>

- THOM, B., HESP, P. & BRYANT, E. (1994), Last glacial “coastal” dunes in Eastern Australia and implications for landscape stability during the Last Glacial Maximum, *Palaeogeography, Palaeoclimatology, Palaeoecology*, 111 (3–4), 229–248, [http://dx.doi.org/10.1016/0031-0182\(94\)90065-5](http://dx.doi.org/10.1016/0031-0182(94)90065-5)
- THOM, B. G. (1983), Transgressive and regressive stratigraphies of coastal sand barriers in southeast Australia, *Marine Geology*, 56 (1–4), 137–158, [http://dx.doi.org/10.1016/0025-3227\(84\)90010-0](http://dx.doi.org/10.1016/0025-3227(84)90010-0)
- THOM, B. G. (1987), Coastal Geomorphology of the Jervis Bay Area, *WETLANDS*, 6 (2), 19–21,
- THOM, B. G., BOWMAN, G. M. & ROY, P. S. (1981), Late Quaternary evolution of coastal sand Barriers, Port Stephens-Myall Lakes Area, central New South Wales, Australia, *Quaternary Research*, 15 (3), 345–364, [http://dx.doi.org/10.1016/0033-5894\(81\)90035-1](http://dx.doi.org/10.1016/0033-5894(81)90035-1)
- THOM, B. G., SHEPHERD, M., LY, C. K., ROY, P. S., BOWMAN, G. M. & HESP, P. A. 1992. *Coastal geomorphology and Quaternary geology of the Port Stephens-Myall Lakes area*, Australian National University, Canberra, ANU.
- THOMPSON, C. H. (1981), Podzol chronosequences on coastal dunes of eastern Australia, *Nature*, 291 (5810), 59–61,
- VARMA, S., SHAH, V., BANERJEE, B. & BUDDHIRAJU, K. (2014), Change Detection of Desert Sand Dunes: A Remote Sensing Approach., *Advances in Remote Sensing*, 3 10–22, 10.4236/ars.2014.31002
- VAZ, D. A., SARMENTO, P. T. K., BARATA, M. T., FENTON, L. K. & MICHAELS, T. I. (2015), Object-based Dune Analysis: Automated dune mapping and pattern characterization for Ganges Chasma and Gale crater, Mars, *Geomorphology*, 250 128–139, <http://dx.doi.org/10.1016/j.geomorph.2015.08.021>
- WASSON, R. J., FITCHETT, K., MACKEY, B. & HYDE, R. (1988), Large-scale patterns of dune type, spacing and orientation in the Australian continental dunefield, *Australian Geographer*, 19 (1), 89–104, 10.1080/00049188808702952
- WASSON, R. J. & HYDE, R. (1983), Factors determining desert dune type, *Nature*, 304 (5924), 337–339,
- WHITEWAY, T. 2009. Australian Bathymetry and Topographic Grid, June 2009. In: OFFICE, G. A. A. T. N. O. (ed.). Geoscience Australia: Geoscience Australia.
- WOOLARD, J. W. & COLBY, J. D. (2002), Spatial characterization, resolution, and volumetric change of coastal dunes using airborne LIDAR: Cape Hatteras, North Carolina, *Geomorphology*, 48 (1–3), 269–287, [http://dx.doi.org/10.1016/S0169-555X\(02\)00185-X](http://dx.doi.org/10.1016/S0169-555X(02)00185-X)
- WORIMI CONSERVATION LANDS 2015. Worimi Conservation Lands Plan of Management Sydney: Office of Environment and Heritage.
- YAN, N. & BAAS, A. C. W. (2015), Parabolic dunes and their transformations under environmental and climatic changes: Towards a conceptual framework for understanding and prediction, *Global and Planetary Change*, 124 123–148, <http://dx.doi.org/10.1016/j.gloplacha.2014.11.010>
- ZHOU, G. & XIE, M. (2009), Coastal 3-D Morphological Change Analysis Using LiDAR Series Data: A Case Study of Assateague Island National Seashore, *Journal of Coastal Research*, 25 (2), 435–447,

Chapter 6: Appendices

Appendix 1: Comparison between Bilinear, Cubic Convolutions and Nearest resampling techniques used to resample Port Stephens and Raymond Terrace DEMs (Note: DEMs were snapped to Hunter DEM cells).

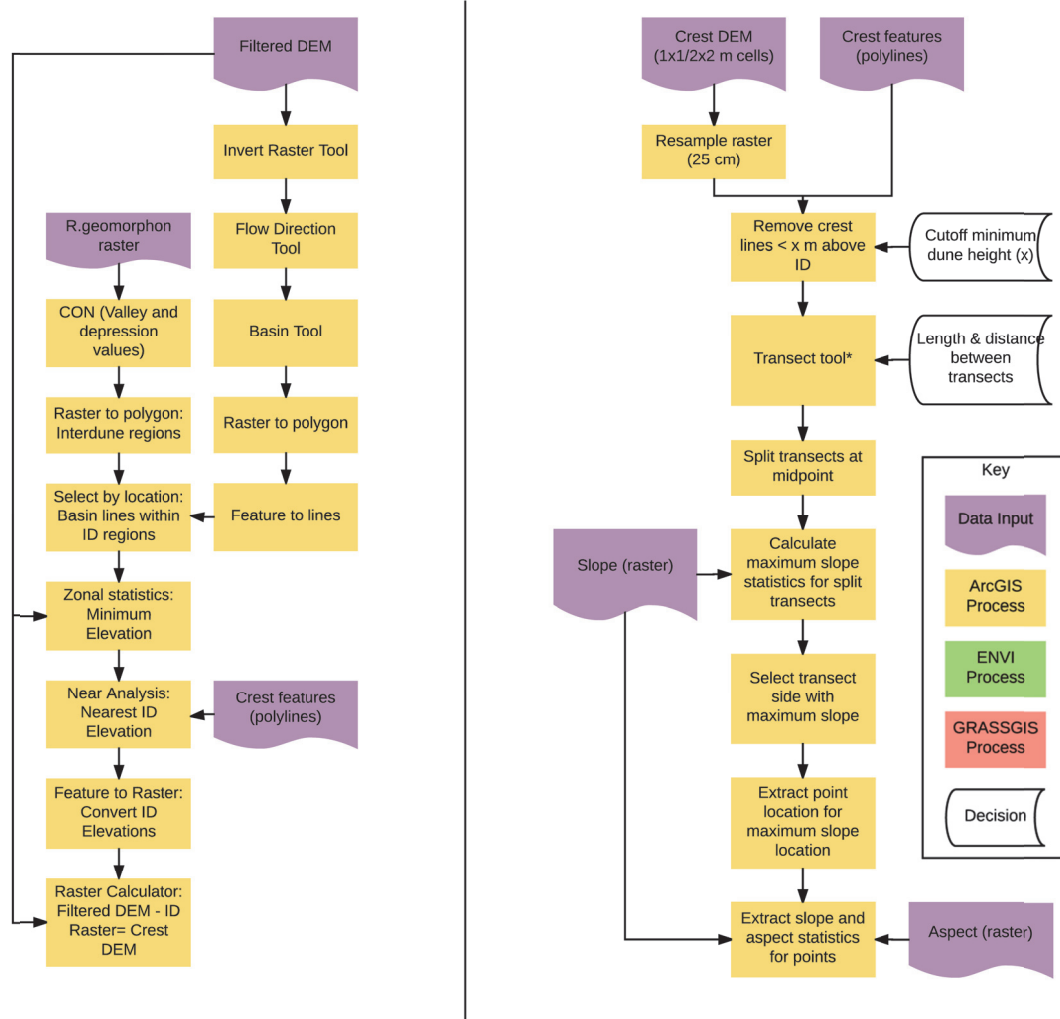
Raymond Terrace DEM

	Minimum Difference (m)	Maximum Difference (m)	Mean Difference (m)	Standard Deviation (m)
Nearest Neighbour	-2.884	2.504	0.00	0.18
Bilinear	-1.60775	1.3635	0.00	0.09
Cubic Convolutions	-1.71257	1.47048	0.00	0.09

Port Stephens DEM

	Minimum Difference (m)	Maximum Difference (m)	Mean Difference (m)	Standard Deviation (m)
Nearest Neighbour	-4.466	4.846	0.00	0.31
Bilinear	-3.4085	4.3075	0.00	0.22
Cubic Convolutions	-3.57391	4.39956	0.00	0.22

Appendix 2: Dune height and orientation methods flow charts



Appendix 3: Von Mises orientation statistics table of modelled modes (integer values between 2-6) for each dune group.

Seal Rocks

All Dunes

2 groups	Proportion	Degree	L	L/L Total
1	0.480037	115.2516	656.8611	0.952846
2	0.519963	287.6206		
3 groups				
1	0.419128	122.8885	676.3417	0.981105
2	0.328688	274.0451		
3	0.252184	0.356838		
4 groups				
1	0.225493	81.02132	678.2901	0.983931
2	0.266862	262.3978		
3	0.28263	134.9022		
4	0.225016	325.1216		

5 groups					
1	0.159393	31.84812	679.5817	0.985805	
2	0.199567	101.9555			
3	0.216032	309.1575			
4	0.207409	253.2104			
5	0.217598	151.1088			

6 groups					
1	0.179145	102.6814	689.3674	1	
2	0.149847	45.88764			
3	0.16737	330.7806			
4	0.133446	216.4653			
5	0.203231	272.5771			
6	0.166961	150.0182			

Bridge Hill

2 groups	Proportion	Degree	L	L/L total	
1	0.401603	266.7527	144.0198	0.953443	
2	0.598398	65.92422			

3 groups					
1	0.271727	28.75004	145.1527	0.960943	
2	0.451563	265.5328			
3	0.276711	103.3292			

4 groups					
1	0.196297	25.94232	145.3567	0.962294	
2	0.199374	281.4701			
3	0.325336	100.4044			
4	0.278993	258.4016			

5 groups					
1	0.144987	22.50328	149.6131	0.990472	
2	0.15058	153.1746			
3	0.189037	307.3575			
4	0.303401	254.8607			
5	0.211994	84.67914			

6 groups					
1	0.132437	21.44281	151.0523	1	
2	0.161316	314.2649			
3	0.133554	234.3176			
4	0.150514	134.3915			
5	0.235815	261.0759			
6	0.186364	78.81179			

Inland Parabolics

2 groups	Proportion	Degree	L	L/L total	
1	0.459702	291.7316	201.6946	0.970374	
2	0.540298	107.9194			

3 groups					
1	0.231118	278.9911	202.1263	0.972451	
2	0.522637	109.4982			
3	0.246246	310.6503			

4 groups					
1	0.193931	331.869	204.1913	0.982386	
2	0.298615	272.786			
3	0.282585	138.0996			
4	0.22487	79.66931			

5 groups					
1	0.130303	203.0038	205.5685	0.989012	
2	0.220199	74.49267			
3	0.224607	129.9266			
4	0.197025	334.8735			
5	0.227866	276.8208			

6 groups					
1	0.168018	273.3245	207.8524	1	
2	0.206721	90.01272			
3	0.125495	41.4281			
4	0.199023	324.0778			
5	0.179225	141.8269			
6	0.121519	216.4948			

Unorganised Network

2 groups	Proportion	Degree	L	L/L total	
1	0.469224	121.6709	409.0145	0.959904	
2	0.530777	284.6561			

3 groups					
1	0.368194	126.1948	415.2858	0.974622	
2	0.348402	275.2916			
3	0.283404	18.10503			

4 groups					
1	0.328545	280.3026	420.5487	0.986973	
2	0.182997	22.82528			
3	0.260522	115.6601			
4	0.227936	172.5855			

5 groups					
1	0.166112	320.4667	421.1716	0.988435	
2	0.195058	270.7218			
3	0.152535	44.69931			
4	0.18165	191.4032			
5	0.304644	120.759			

6 groups					
1	0.178117	149.5257	426.0993	1	
2	0.131993	34.62018			
3	0.138161	210.0829			
4	0.175737	270.7634			
5	0.217965	106.4441			
6	0.158028	321.1371			

Coastal Parabolics

2 outputs	Proportion	Degree	L	L/L Total	
1	0.475225	113.6119	347.5537	0.970006	
2	0.524775	300.0316			

3 outputs					
1	0.33261	110.7473	353.6318	0.986969	
2	0.233335	114.1367			
3	0.434056	299.6653			
4 outputs					
1	0.339883	115.5286	355.3122	0.991659	
2	0.367398	300.8772			
3	0.154076	45.22675			
4	0.138643	210.8628			
5 outputs					
1	0.183523	142.6897	357.9142	0.998921	
2	0.211364	268.7646			
3	0.240399	109.0593			
4	0.129532	37.42819			
5	0.235182	311.2089			
6 outputs					
1	0.098264	229.9307	358.3007	1	
2	0.2543	106.4423			
3	0.117058	35.58334			
4	0.153955	141.2031			
5	0.196599	286.663			
6	0.179823	317.3234			

Foredune Complex

2 groups	Proportion	Degree	L	L/L total	
1	0.470593	311.7293	491.9079	0.880381	
2	0.529407	131.2288			
3 groups					
1	0.11722	157.9984	537.1044	0.961271	
2	0.513691	308.8007			
3	0.369089	117.5165			
4 groups					
1	0.416596	298.4888	550.2383	0.984777	
2	0.166759	318.1433			
3	0.148036	157.2308			
4	0.268609	110.789			
5 groups					
1	0.282186	275.5444	553.3173	0.990288	
2	0.196123	155.5964			
3	0.216388	321.1379			
4	0.145788	74.15665			
5	0.159515	109.1501			
6 groups					
1	0.225846	109.1853	558.7441	1	
2	0.186027	327.0447			
3	0.184271	155.959			
4	0.137374	34.84248			
5	0.168849	283.9234			
6	0.097633	213.6318			

Newcastle Bight

All Dunes

2 groups	Proportion	Degree	L	L/L Total
1	0.485737	110.549	791.7374	0.912566
2	0.514263	284.0382		
3 groups			L	
1	0.269825	96.66077	818.7364	0.943685
2	0.443248	296.1274		
3	0.286928	159.4		
4 groups				
1	0.287197	270.2163	858.004	0.988946
2	0.201159	350.3332		
3	0.199081	88.69829		
4	0.312563	151.0348		
5 groups				
1	0.211691	86.63921	867.1745	0.999516
2	0.231854	143.3049		
3	0.166766	219.6647		
4	0.159925	2.948369		
5	0.229765	287.3528		
6 groups				
1	0.225957	86.54255	867.5946	1
2	0.154819	2.374129		
3	0.187864	141.5773		
4	0.122594	238.7275		
5	0.112888	191.3023		
6	0.195879	290.7827		

First Generation

2 groups	Proportion	Degree	L	L/L Total
1	0.609019	260.4147	126.7332	0.805519
2	0.390981	89.24861		
3 groups				
1	0.380694	282.0434	135.0721	0.858521
2	0.25615	85.15632		
3	0.363157	199.7427		
4 groups				
	0.270183	162.8742	155.786	0.990179
	0.328334	266.1804		
	0.206932	10.35304		
	0.194551	86.05327		
5 groups				
1	0.228817	282.336	157.1509	0.998854
2	0.176758	11.79086		
3	0.221351	85.58217		
4	0.185168	224.7351		
5	0.187906	153.2385		

6 groups

1	0.240062	85.20688	157.3312	1
2	0.166826	151.1947		
3	0.127918	309.1445		
4	0.141431	13.928		
5	0.151802	211.8618		
6	0.17196	268.6575		

Second Generation

2 groups	Proportion	Degree	L	L/L Total
1	0.6011	250.0173	393.971	0.92966
2	0.3989	107.2376		
3 groups				
1	0.40416	186.0581	414.84	0.978906
2	0.25137	96.95203		
3	0.34447	302.8639		
4 groups				
1	0.17614	353.6856	418.943	0.988589
2	0.33835	98.4344		
3	0.27018	184.7229		
4	0.21533	269.5409		
5 groups				
1	0.15083	0.559612	423.42	0.999153
2	0.21091	205.4097		
3	0.23421	134.3503		
4	0.20624	86.04837		
5	0.1978	280.2907		
6 groups				
1	0.19607	85.02993	423.779	1
2	0.12626	272.4069		
3	0.22189	131.722		
4	0.19576	200.1534		
5	0.12509	285.2478		
6	0.13492	5.647691		

Beach Ridges

2 groups	Proportion	Degree	L	L/L Total
1	0.564661	343.6413	524.6226	0.840928
2	0.435339	160.2427		
3 groups				
1	0.196146	352.4021	581.1379	0.931517
2	0.394222	160.396		
3	0.409632	337.0667		
4 groups				
1	0.134307	172.009	612.6464	0.982023
2	0.391723	334.3213		
3	0.290893	150.8618		
4	0.183077	353.4497		

5 groups

1	0.093641	133.2001	622.1198	0.997208
2	0.23776	171.3751		
3	0.198805	355.1925		
4	0.31057	356.1127		
5	0.159225	326.6857		

6 groups

1	0.108664	179.8425	623.8617	1
2	0.20306	112.2915		
3	0.288637	331.4804		
4	0.107544	167.9785		
5	0.113988	137.0023		
6	0.178107	354.2925		

Current Generation South

2 groups	Proportion	Degree	L	L/L Total
1	0.555647	113.104	239.0575	0.856632
2	0.444353	284.3368		
3 groups				
1	0.225596	6.26833	256.6462	0.919659
2	0.488347	120.43		
3	0.286058	268.7678		
4 groups				
1	0.2019	144.3055	265.0449	0.949754
2	0.357048	266.1776		
3	0.174277	7.844832		
4	0.266774	95.35927		
5 groups				
1	0.276783	270.2207	273.6663	0.980648
2	0.101507	146.6912		
3	0.178957	1.29927		
4	0.323917	101.2396		
5	0.118837	186.9587		
6 groups				
1	0.162777	257.6512	279.0668	1
2	0.284454	101.4251		
3	0.095393	146.3176		
4	0.123996	172.6579		
5	0.18236	297.5361		
6	0.151021	26.55857		

Current Generation North

2 groups	Proportion	Degree	L	L/L Total
1	0.474319	290.7572	633.1819	0.979436
2	0.525682	103.0796		

3 groups					
1	0.373093	99.64072	635.8151	0.983509	
2	0.235791	135.5834			
3	0.391116	293.0716			
4 groups					
1	0.148537	13.75696	637.1041	0.985503	
2	0.235832	130.4429			
3	0.225646	91.89706			
4	0.389985	289.3828			
5 groups					
1	0.250381	90.46581	645.0734	0.99783	
2	0.274893	298.0438			
3	0.187947	140.2446			
4	0.145162	241.7934			
5	0.141617	18.44496			
6 groups					
1	0.125193	233.1059	646.476	1	
2	0.141826	45.30932			
3	0.22448	93.96734			
4	0.165729	144.6991			
5	0.179091	287.1981			
6	0.163681	320.0032			

Booderee

All Dunes

2 groups	Proportion	Degree	L	L/L Total	
1	0.481817	275.1133	432.4248	0.942827	
2	0.518183	108.6405			
3 groups					
1	0.433617	281.9493	444.0399	0.968151	
2	0.326411	144.2368			
3	0.239972	91.81849			
4 groups					
1	0.161826	358.0996	454.0734	0.990028	
2	0.266115	93.14797			
3	0.250363	165.6303			
4	0.321697	273.7635			
5 groups					
1	0.202558	151.9838	456.6841	0.99572	
2	0.222263	281.9663			
3	0.260804	89.34413			
4	0.154937	356.4111			
5	0.159439	225.7471			

6 groups

1	0.142612	336.9865	458.6472	1
2	0.12719	60.28562		
3	0.199445	278.5406		
4	0.146081	222.0982		
5	0.157306	159.1632		
6	0.227367	98.75586		

Parabolic Generation One

2 groups	Proportion	Degree	L	L/L Total
1	0.458327	90.3311	148.35	0.941638
2	0.541673	261.259		
3 groups				
1	0.324637	221.6236	153.6699	0.975405
2	0.239647	283.3265		
3	0.435715	84.63974		
4 groups				
1	0.15684	19.15685	156.6815	0.994521
2	0.249992	205.7796		
3	0.250902	280.5157		
4	0.342266	92.59258		
5 groups				
1	0.179789	204.9264	156.9568	0.996268
2	0.217807	87.02058		
3	0.295036	279.0062		
4	0.149257	125.6754		
5	0.158111	22.47917		
6 groups				
1	0.130884	28.10378	157.5447	1
2	0.191509	268.6701		
3	0.190709	81.84616		
4	0.174857	204.4618		
5	0.172081	127.521		
6	0.139962	305.6235		

Parabolic Generation 2

2 groups	Proportion	Degree	L	L/L total
1	0.477971	103.7884	465.4414	0.974252
2	0.522029	267.133		
3 groups				
1	0.328762	160.7505	470.1223	0.98405
2	0.347247	274.1324		
3	0.323992	99.08598		

4 groups

1	0.134282	4.056269	473.5285	0.991179
2	0.227686	213.2726		
3	0.237882	280.7841		
4	0.400151	102.7698		

5 groups

1	0.244894	91.71798	476.9025	0.998242
2	0.123741	16.23925		
3	0.201818	138.9109		
4	0.236097	286.2232		
5	0.19345	227.0474		

6 groups

1	0.105935	40.68057	477.7425	1
2	0.201601	281.6359		
3	0.096948	322.7306		
4	0.176133	223.3413		
5	0.177254	142.8633		
6	0.242128	94.52355		

Appendix 4: Height statistics by dune group

Site	Generation/Dune Type	Minimum Height (m)	Max Height (m)	Mean Height (m)	Standard Deviation	Count (# of cells)
BOO	All Dunes	1	35.30	4.78	3.97	256282
BOO	Beach Ridges	1	7.97	1.90	1.03	12856
BOO	Parabolic Gen 1	1	31.75	4.83	3.98	91987
BOO	Parabolic Gen 2	1	35.30	5.00	4.02	151439
NCB	All Dunes	1	45.08	5.43	5.18	390546
NCB	Beach Ridges	1	9.98	2.44	1.26	21195
NCB	Current Gen	1	38.49	6.24	4.95	147898
NCB	Current Gen South	1	21.24	5.05	4.00	39779
NCB	Current Gen North	1	38.49	6.67	5.19	108161
NCB	Second Gen	1	37.96	4.96	4.99	140952
NCB	First Gen	1	45.08	5.55	6.12	80455
SR	All Dunes	1	99.98	6.64	7.13	637597
SR	Foredune All	1	33.08	5.06	3.78	85284
SR	Foredune Parabolic	1	33.08	5.58	3.78	63461
SR	Inland Parabolic	1	60.36	9.29	7.92	112200
SR	Parabolic All	1	60.36	7.95	6.96	175661
SR	Unorganised Network	1	99.98	4.80	5.37	230736
SR	Transverse	1	43.26	6.46	6.33	176718
SR	Bridge Hill	1	91.70	14.07	12.16	49734

Appendix 5: Volumetric analysis of study dunefields- table of derived volumes.

Dunefield	Group	Area (m ²)	Volume (m ³)	Percent of Total Dunefield Volume (%)
Seal Rocks	Bridge Hill	7000100	222271612.2	35.70
	Transverse Dunes	13702655	137086301.3	22.02
	Inland Parabolics	7293637	112498481.8	18.07
	Unorganised Network	17035860	137584007	22.10
	Foredune Complex	3884593	13182872.05	2.12
	Total Dunefield	4891685	622623274.3	100.00
Newcastle Bight	First Generation	15436684	86088705.62	18.00
	Second Generation	17957276	133742700.4	27.97
	Beach Ridges	5053536	30528362.96	6.38
	Current Generation South	7949328	41394725.71	8.66
	Current Generation North	19520316	186433779.5	38.99
	Total Dunefield	65917140	478188274.2	100
Booderee	First Generation Parabolics	4544472	26002121.18	25.40
	Second Generation Parabolics	7135557	50745870.39	49.58
	Beach Ridges	567098	1550213.456	1.51
	Other (Rehabilitated Foredune)	2758201	24057246.25	23.50
	Total Dunefield	15005328	102355451.3	100.00

Appendix 6: RDD graphs for Autumn and Spring during the study period January 2007-July 2013 (created using daily RDD data). The arrows represent the median RDD for each period. **Note:** The rose plots have different frequency scales to improve legibility. Created from wind data collected by the Bureau of Meteorology from Williamtown AWS.

